APPLICATION FOR FEDERAL ASSISTANCE
SF 424 (R&R)

2. DATE SUBMITTED 03/25/2008	**Applicant Identifier** 089634 Catalano, J
3. DATE RECEIVED BY STATE	**State Application Identifier**

1. * TYPE OF SUBMISSION

○ Pre-application   ● Application
  ○ Changed/Corrected Application

4. Federal Identifier

5. APPLICANT INFORMATION
* Organizational DUNS: 068552207

* Legal Name: Washington University
Department: RESEARCH OFFICE   Division: Vice Chancellor for Research
* Street1: Campus Box 1054   Street2: One Brookings Drive
* City: St. Louis   County: St. Louis   * State: MO: Missouri
Province: * Country: USA: UNITED STATES   * ZIP / Postal Code: 63130

Person to be contacted on matters involving this application

Prefix:	* First Name:	Middle Name:	* Last Name:	Suffix:
Ms	Kaaren	J	Downey	

* Phone Number: (314) 935-5889   Fax Number: (314) 935-5862   Email: HOLLERAN@LEVEE.WUSTL.EDU

6. * EMPLOYER IDENTIFICATION NUMBER (EIN) or (TIN):
1-43-065-3611A1

7. * TYPE OF APPLICANT
O: Private Institution of Higher Education

8. * TYPE OF APPLICATION: ● New

○ Resubmission   ○ Renewal   ○ Continuation   ○ Revision

Other (Specify):
Small Business Organization Type
○ Women Owned   ○ Socially and Economically Disadvantaged

If Revision, mark appropriate box(es).

○ A. Increase Award   ○ B. Decrease Award   ○ C. Increase Duration
○ D. Decrease Duration ○ E. Other (specify):

* Is this application being submitted to other agencies? ○ Yes ● No
What other Agencies?

9. * NAME OF FEDERAL AGENCY:
DEPARTMENT OF ENERGY

10. CATALOG OF FEDERAL DOMESTIC ASSISTANCE NUMBER:
TITLE:

11. * DESCRIPTIVE TITLE OF APPLICANT'S PROJECT:
PHOSPHATE CONTROLS ON SUBSURFACE URANIUM FATE AND TRANSPORT: CONNECTING MOLECULAR-SCALE AND SEDIMENT

12. * AREAS AFFECTED BY PROJECT (cities, counties, states, etc.)
N/A

13. PROPOSED PROJECT:

* Start Date	* Ending Date
09/01/2008	08/31/2011

14. CONGRESSIONAL DISTRICTS OF:

a. * Applicant	b. * Project
MO3	MO3

15. PROJECT DIRECTOR/PRINCIPAL INVESTIGATOR CONTACT INFORMATION

Prefix:	* First Name:	Middle Name:	* Last Name:	Suffix:
Dr	Jeffrey	G.	Catalano	

Position/Title: Assistant Professor of Earth and Pl   * Organization Name: Washington University
Department: EARTH AND PLANETARY SCIENCES   Division: SCHOOL OF ARTS & SCIENCES
* Street1: Campus Box 1169   Street2: One Brookings Drive
* City: St. Louis   County: St. Louis   * State: MO: Missouri
Province: * Country: USA: UNITED STATES   * ZIP / Postal Code: 63130
* Phone Number: 314/935-6015   Fax Number: 314/935-7361   * Email: catalano@levee.wustl.edu

16. ESTIMATED PROJECT FUNDING		17. * IS APPLICATION SUBJECT TO REVIEW BY STATE EXECUTIVE ORDER 12372 PROCESS?
a. * Total Estimated Project Funding	$931,543.00	a. YES ○ THIS PREAPPLICATION/APPLICATION WAS MADE AVAILABLE TO THE STATE EXECUTIVE ORDER 12372 PROCESS FOR REVIEW ON:
b. * Total Federal & Non-Federal Funds	$931,543.00	DATE:
c. * Estimated Program Income	$0.00	b. NO ● PROGRAM IS NOT COVERED BY E.O. 12372; OR
		○ PROGRAM HAS NOT BEEN SELECTED BY STATE FOR REVIEW

18. By signing this application, I certify (1) to the statements contained in the list of certifications* and (2) that the statements herein are true, complete and accurate to the best of my knowledge. I also provide the required assurances * and agree to comply with any resulting terms if I accept an award. I am aware that any false, fictitious, or fraudulent statements or claims may subject me to criminal, civil, or administrative penalties. (U.S. Code, Title 18, Section 1001)

● * I agree

* The list of certifications and assurances, or an Internet site where you may obtain this list, is contained in the announcement or agency specific instructions.

19. Authorized Representative

Prefix: * First Name: Middle Name: * Last Name: Suffix:

Ms   Kaaren   J   Downey

* Position/Title: Assistant Director   * Organization Name: Washington University

Department: RESEARCH OFFICE   Division: Vice Chancellor for Research

* Street1: Campus Box 1054   Street2: One Brookings Drive

* City: St. Louis   County: St. Louis   * State: MO: Missouri

Province: * Country: USA: UNITED STATES   * ZIP / Postal Code: 63130

* Phone Number: (314) 935-5889   Fax Number: (314) 935-5862   * Email: resoffice@msnotes.wustl.edu

* Signature of Authorized Representative   *** Date Signed**

03/25/2008

20. Pre-application   File Name: Mime Type:

21. Attach an additional list of Project Congressional Districts if needed.

File Name: Mime Type:

RESEARCH & RELATED Other Project Information

1. * Are Human Subjects Involved? ⭘ Yes ● No	

1.a. If YES to Human Subjects

Is the IRB review Pending? ⭘ Yes ⭘ No

IRB Approval Date:

Exemption Number: ▬ 1 ▬ 2 ▬ 3 ▬ 4 ▬ 5 ▬ 6

Human Subject Assurance Number

---

2. * Are Vertebrate Animals Used? ⭘ Yes ● No

2.a. If YES to Vertebrate Animals

Is the IACUC review Pending? ⭘ Yes ⭘ No

IACUC Approval Date:

Animal Welfare Assurance Number

---

3. * Is proprietary/privileged information ⭘ Yes ● No

included in the application?

4.a. * Does this project have an actual or potential impact on ⭘ Yes ● No
the environment?

4.b. If yes, please explain:

4.c. If this project has an actual or potential impact on the environment, has an exemption been authorized or an environmental assessment (EA) or environmental impact statement (EIS) been performed? ⭘ Yes ⭘ No

4.d. If yes, please explain:

5.a. * Does this project involve activities outside the U.S. or ⭘ Yes ● No
partnership with International Collaborators?

5.b. If yes, identify countries:

5.c. Optional Explanation:

---

6. * Project Summary/Abstract	
7. * Project Narrative	089634Catalano_DOE_ERSP_package.pdf Mime Type: application/pdf
8. Bibliography & References Cited	
9. Facilities & Other Resources	
10. Equipment	

Phosphate Controls on Subsurface Uranium Fate and Transport: Connecting Molecular-Scale and Sediment-Scale Processes

Jeffrey G. Catalano[1] (PI), Daniel E. Giammar[1], Dawn M. Wellman[2]

1. Washington University, St. Louis, MO
2. Pacific Northwest National Laboratory, Richland, WA

PROJECT SUMMARY

Widespread subsurface uranium contamination at DOE sites has resulted from historical deliberate and accidental discharge of nuclear waste into the environment. The occurrence of uranyl phosphate solids in contaminated subsurface regions at several sites and the expected formation of additional uranyl phosphates during pilot testing of a new treatment method in the Hanford 300 Area demonstrate that these phases play an important role in controlling the environmental fate and transport of uranium at many DOE facilities. *A fundamental understanding of the formation of uranyl phosphates and their long-term stability in subsurface environments is needed to assess the role of phosphate in long-term stewardship and provide the scientific basis for phosphate-induced remediation strategies*.

The overall objective of the proposed research is to advance the scientific basis of uranyl phosphate formation and long-term stability. Specific objectives are to: (1) *Determine the geochemical factors governing uranyl phosphate formation in the subsurface*; and (2) *Evaluate the long-term stability of uranyl phosphates formed in the subsurface*. To meet these objectives, the proposed research approach will test the following hypotheses: (1) Molecular interactions in solution and at mineral surfaces control the phases that form in systems supersaturated with respect to uranyl phosphate solids; (2) These molecular-scale interactions and the degree of water saturation govern the spatial distribution and precipitation rates of uranyl phosphates in heterogeneous porous media; (3) The solution composition will control uranyl phosphate dissolution rates as a result of molecular-scale factors that govern variations in dissolution mechanisms and the formation of secondary solid phases; (4) Rates of uranyl phosphate dissolution and secondary phase formation can be used to predict the net release rate of U(VI) from phosphate-treated heterogeneous porous media; (5) As result of wetting-drying cycles and increased reactive surface area, the formation of secondary phases and the net rate of U(VI) release will be accelerated under water-unsaturated conditions.

Our team will test these hypotheses through a research approach that progresses from the molecular-scale to the sediment-scale in two integrated modules. In both modules, the approach will (a) apply techniques to gain molecular-scale insights into reaction mechanisms, (b) quantify rates and mechanisms of processes in controlled laboratory systems, and (c) assess the role of these processes in controlling uranium fate and transport in porous media, specifically in Hanford sediments. Module I will investigate the formation of uranyl phosphate solids in heterogeneous systems in tasks that examine (1) nucleation on pure mineral surfaces, (2) precipitation in batch and column reactors loaded with Hanford sediments, and (3) uranium speciation in phosphate-treated sediments from a field test site. Module II will examine the processes that control the long-term stability of uranyl phosphates in tasks that (1) probe the mechanisms of dissolution at the nanoscale, (2) quantify macroscale dissolution rates, and (3) assess the impact of dissolution on the net rate of release from Hanford sediments at saturated and unsaturated conditions. These studies will serve as a foundation for the development of a robust conceptual model to describe the effects of phosphate on the environmental fate and transport of U(VI).

The proposed project will support the ERSD mission by advancing the scientific understanding of processes that control uranium fate and transport in subsurface systems. The project will provide the scientific basis for credibly predicting the formation and long-term stability of uranyl phosphates in the subsurface at important DOE sites. Key molecular-scale mechanisms involved in uranyl phosphate formation and long-term stability will be characterized, and the effects of these mechanisms on sediment-scale processes will be determined. This knowledge is required for effective application of new remediation strategies that will mitigate the environmental impact of past nuclear activities.

Phosphate Controls on Subsurface Uranium Fate and Transport: Connecting Molecular-Scale and Sediment-Scale Processes

Full Proposal Submitted to DE-PS02-08ER08-09

Is this an Exploratory Proposal?   No   .

Principal Investigator (name, affiliation, phone, e-mail)

Jeffrey Catalano
Washington University, Earth and Planetary Sciences
(314) 935-6015
catalano@levee.wustl.edu

Funded Co-Investigators (name, affiliation, phone, e-mail)

Daniel Giammar
Washington University, Chemical Engineering
(314) 935-6849
Giammar@wustl.edu

Dr. Dawn M. Wellman
Environmental Technology Directorate
Pacific Northwest National Laboratory
PO Box 999, Richland, WA 99352
Tel.: (509) 375-2017
E-mail: Dawn.Wellman@pnl.gov

Unfunded Collaborators (name, affiliation, phone, e-mail)

Requested Funding (not required for pre-applications)

Institution	FY 2009	FY 2010	FY 2011	Total
Washington U-Catalano				
Washington U-Giammar				
PNNL-Wellman				
Total				

I. INTRODUCTION

Widespread subsurface uranium contamination at DOE sites has resulted from historical deliberate and accidental discharge of nuclear waste into the environment. For example, waste disposal into unlined trenches and storage ponds and leakage from single-shell tanks has resulted in plumes of uranium(VI) in groundwater at the Hanford Site and Oak Ridge Reservation. A sizeable groundwater plume beneath the Hanford 300 Area adjacent to the Columbia River has received much attention in recent years [1,2]. Remedial strategies are currently being evaluated and models are under development to credibly predict U(VI) fate and transport at this site.

Uranyl phosphate solids are common forms of U(VI) in contaminated soils and sediments at DOE facilities, most notably in the vadose zone of the Hanford 300 Area. Solid-phase uranium sources in the vadose zone of the 300 Area are sustaining the large groundwater plume [2]. Uranium species in the source-term have been identified as U(VI) adsorbed onto phyllosilicate surfaces and as uranyl phosphate minerals [3,4]. Additional uranyl phosphates are expected to form at this site during pilot testing of a new polyphosphate treatment method intended to remediate the elevated uranium concentrations in groundwater [5]. This remediation approach is motivated by the low solubility of uranyl phosphates, which often are the lowest solubility U(VI) phases in natural environments [6] and may have greater long-term stability in oxic groundwaters than U(IV) oxides produced during bioremediation [7,8]. Phosphate addition is also being explored to enhance the stability of uranium immobilized by reductive bioremediation at the Oak Ridge Field Research Center; the phosphate may protect against release resulting from reoxidation [9]. Even without phosphate addition, uranyl phosphates have been observed in contaminated soils and sediments at the Oak Ridge Reservation [10,11] and at the Fernald Site [12-14].

The frequent occurrence of uranyl phosphate solids in contaminated subsurface regions and the expected formation of additional uranyl phosphates during pilot testing of a new treatment method in the Hanford 300 area demonstrate that these phases play an important role in controlling the environmental fate and transport of uranium at many DOE facilities. *A fundamental understanding of the formation of uranyl phosphates and their stability in subsurface environments is needed to assess the role of phosphate in long-term stewardship and provide the scientific basis for phosphate-induced remediation strategies*. This understanding is currently lacking in key areas. *The formation mechanism, identity, and location of uranyl phosphate phases precipitated in sediments following phosphate addition are generally unknown*. In sediments, the presence of substrate mineral surfaces (e.g., feldspars and clays) can influence the rates and mechanisms of uranyl phosphate formation. Subsequent mineral transformations can be induced by wetting-drying cycles and reactions with groundwater cations. *For uranyl phosphates formed in the subsurface, questions remain regarding their long-term stability*. While dissolution rates of autunite minerals have been quantified under some conditions, these minerals display nonstoichiometric dissolution, with substantially more phosphate release than U(VI) release; the dissolution mechanism(s) and the nature of the remaining U(VI)-enriched solid phase are still unknown [15,16].

1

II. PROJECT OBJECTIVES

The overall objective of the proposed research is to advance the scientific basis of uranyl phosphate formation and long-term stability to provide improved estimates of the environmental fate and transport of uranium in the subsurface. Meeting this objective will involve advances in our understanding of the factors that control uranyl phosphate formation, stability, and dissolution from the molecular-scale to the sediment-scale. Specific objectives are:

A. Objective 1: Determine the geochemical factors governing uranyl phosphate formation in the subsurface.

- Determine if heterogeneous nucleation of uranyl phosphates on mineral surfaces alters the phase that forms, and evaluate how this processes affects the distribution of uranyl phosphates in sediments.

- Evaluate the role of solution composition, water saturation, and mineral components on uranyl phosphate precipitation in Hanford sediments, and develop a reaction-based conceptual model of uranyl phosphate formation in heterogeneous porous media.

- Characterize the speciation and distribution of uranyl phosphate precipitates in sediments from a phosphate injection test site.

B. Objective 2: Evaluate the long-term stability of uranyl phosphates formed in the subsurface.

- Determine the mechanisms and rates of dissolution and transformation processes of uranyl phosphates at the nanoscale.

- Quantify the macroscopic dissolution rates of uranyl phosphates, identify the products of nonstoichiometric dissolution, and correlate measured rates with nanoscale mechanisms

- Evaluate the rates of uranyl phosphate dissolution in Hanford sediments under water-saturated and unsaturated conditions.

III. SCIENTIFIC BACKGROUND

The relevant scientific literature is reviewed below to support the major hypotheses to be tested and to motivate the experimental design. The hypotheses and research follow in Section IV.

A. Geochemistry of Relevant Contaminated Sites

The subsurface geochemistry at several uranium-contaminated DOE sites, including the Hanford 300 Area, is conducive to uranyl phosphate formation. Uranyl phosphates, primarily the mineral autunite [$Ca(UO_2)_2(PO_4)_2 \cdot 11H_2O$], were identified in uranium-contaminated soils at the Fernald site in Ohio [12-14]. Roh et al. [10] identified a Ca-U-phosphate, nominally autunite, in contaminated soils at the DOE–K 25 site at the Oak Ridge Reservation. Uranyl phosphate solids were also identified in sediments from the NABIR FRC at Oak Ridge [11]. A recent spectroscopic study nominally agreed with this identification [17]. Uranium stabilization through uranyl phosphate precipitation induced by the microbial degradation of organo-phosphate compounds is being explored as a treatment method in the subsurface at this site [9,18]. Uranyl phosphates have been identified in contaminated vadose zone sediments from the Hanford 300 Area [3,4], and treatment methods are being tested that encourage further formation

of these phases [5]. *Uranyl phosphates are thus key species at many DOE sites with subsurface uranium contamination.*

The most relevant site to this proposal is the 300 Area at the south end of the Hanford Site. Waste disposal ponds approximately 100 m west of the Columbia River received basic sodium aluminate and acidic U(VI)-Cu(II) waste streams from the dissolution of nuclear fuel and fuel rod cladding from 1943 to 1975. The two ponds received approximately 58,000 kg of U; 238,000 kg of Cu; 1,156,000 kg of F^-; 243,000 kg of NO_3^-; large amounts of Al as $Al(OH)_4^-$; and lesser undocumented amounts of Ni, Cr, Zn, and P. The pH of the pond water was temporally variable, ranging from 1.8 to 11.4. Sodium hydroxide was frequently added when the pH was acidic to minimize leaching of Cu and U through the vadose zone into the underlying unconfined aquifer. Waste disposal nevertheless

Figure 1. *Map of the 300 Area uranium plume in August-September 2001 and the location of the polyphosphate pilot-scale test.*

resulted in a groundwater plume of uranium (**Fig. 1**) [19]. Groundwater from beneath the ponds is slightly alkaline (pH 7.7 to 8.1) with a total ionic strength of 4 to 8 mmol/L. The dominant cations, in order of concentration, are Na^+, Ca^{2+}, and Mg^{2+}, and the dominant anions are HCO_3^-, Cl^-, SO_4^{2-}, and NO_3^-. P_{CO2} values range from 10^{-3} to $10^{-2.5}$, and the groundwater is nominally in equilibrium with calcite. While spatially variable (see **Fig. 1**), U(VI) concentrations typically range from 0.1 to 5 μmol/L (24-1200 μg/L) [2].

Although most uranium-rich sediments from the processes ponds and associated disposal trenches were removed during remedial activities in the late 1990s, the size and uranium concentrations in this groundwater plume have remained unchanged over the last decade. The current conceptual model for the site [1] holds that residual uranium in lower vadose zone and capillary fringe sediments is slowly desorbing. This desorption is enhanced when the Columbia River is at high stage, which results in groundwater flow into the unconfined aquifer, raising the water table and exposing more uranium-bearing materials to saturated conditions. The highest uranium groundwater concentrations in recent years occurred during times with exceptionally high water levels in the Columbia River, suggesting that the remaining pool of uranium is substantial and that future wet years will produce high uranium groundwater concentrations.

Recent studies have investigated the solid-phase vadose zone source term that is suspected of sustaining the groundwater plume. *Uranium predominantly occurs adsorbed to phyllosilicates and precipitated as autunite group uranyl phosphate minerals in the Hanford 300 Area vadose zone* [4]. X-ray microdiffraction (μ-XRD) measurements suggest that the phosphate phase is the mineral metatorbernite [$Cu(UO_2)_2(PO_4)_2 \cdot 8H_2O$], an autunite group mineral [3]. It was also suggested that β-uranophane was present, but this assignment is problematic as the main μ-XRD peak used for this determination (d-spacing of 3.33 Å) is more likely to be from quartz (strongest line at 3.34 Å). Treatment methods for the site are currently under investigation (see Section III.B.).
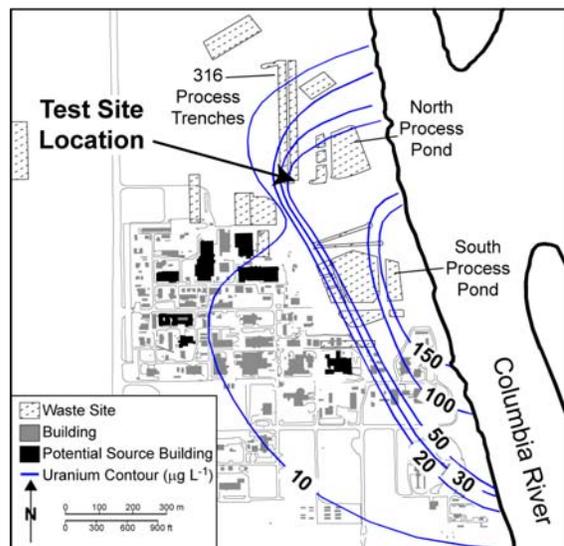
B. Uranium Immobilization Through In Situ Polyphosphate Treatment

Polyphosphate addition has recently been demonstrated to be an effective treatment method by inducing the formation of uranyl phosphate solids [20,21]. Injection of orthophosphate (PO_4^{3-}) into subsurface systems is not normally effective because it can cause precipitation of mineral phases such as apatite [$Ca_5(PO_4)_3OH$] near the point of injection, drastically altering the hydraulic conductivity. Injection of polyphosphates delays the formation of minerals until the polyphosphate degrades to yield orthophosphate (**Fig. 2**). This degradation and precipitation typically occurs after the polyphosphate has dispersed into the aquifer system, leading to in situ sequestration of uranium over a wide area.

A site-specific treatability test was conducted to optimize polyphosphate remediation technology for implementation through a pilot-scale field technology demonstration. The technology can accelerate natural attenuation of the uranium plume within the Hanford 300 Area aquifer [16,22-24]. Focused application of polyphosphate was conducted in a source or "hot spot" area to reduce the inventory of available uranium through direct precipitation of uranyl phosp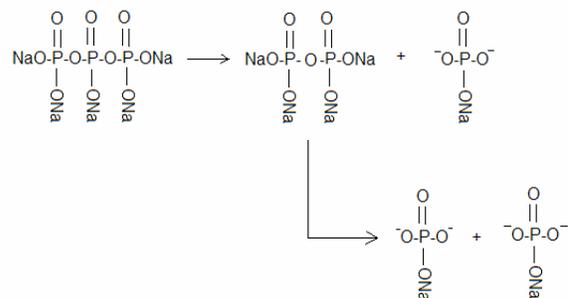hate solids and secondary containment via precipitation of apatite, which acts as a long-term sorbent for uranium [25]. The field test was conducted at a Hanford 300 Area location containing the highest uranium concentrations (>120 µg/L) in the plume (**Fig. 1**). Well 399-1-23 was selected for the treatability test [26]. This well is located at the southern end of a waste disposal trench that is a known source of uranium. The well is sufficiently inland from the Columbia River that infiltration of river water during most high discharge conditions does not reach the well. This well also was selected because of it has a moderately thick (~6.1 m) interval of contaminated permeable Hanford gravel below the water table. Depth-discrete uranium concentrations in groundwater samples collected during drilling were highest in the uppermost portion of the aquifer and decreased to below detection deep in the aquifer below the contact between the Hanford and Ringold formations.

Figure 2. *The step-wise hydrolysis of sodium tripolyphosphate*

Prior to polyphosphate remediation the aqueous concentration of uranium ranged from ~50 to 110 µg/L. Data obtained a week after the treatment indicated a substantial reduction in uranium concentrations in most wells within the targeted and extended treatment zones. The average post-treatment uranium concentration was 28 µg/L after one week and 19 µg/L after two weeks as compared to the average pretreatment concentration of 79 µg/L. Preliminary field data indicate that polyphosphate injection technology has the potential to effectively capture and sequester uranium from contaminated groundwater plumes resulting in the reduction of uranium concentrations to below the EPA MCL of 30 µg/L. *However, the molecular-scale mechanisms responsible for this reduction in aqueous uranium concentrations are unknown. Knowledge of these mechanisms is important for optimizing remediation approaches and predicting the long-term stability of the immobilized uranium.* Now after 9 months, aqueous uranium concentrations at the majority of the wells within the treatment and extended treatment zone remain well below the average baseline concentration. Current research is focusing on utilizing polyphosphate technology to treat the source of uranium within the vadose zone and capillary fringe in the Hanford 300 Area [27]. Because the rates and mechanisms of reactions at the solid-water

interface can vary with the degree of water saturation **[28,29]**, the role of unsaturated conditions on phosphate-based immobilization is an important knowledge gap to be filled.

C. Aqueous Geochemistry and Mineralogy of Uranium(VI) in Environmental Systems

U(VI) is known to display complex speciation in natural waters, forming aqueous complexes of UO_2^{2+} with OH^-, CO_3^{2-}, PO_4^{3-}, SO_4^{2-}, $H_4SiO_{4(aq)}$, F^-, Cl^-, and NO_3^- **[30-33]**. In addition, U(VI) has recently been shown to form ternary UO_2^{2+}-CO_3^{2-}-X^{2+} complexes in solution, where X^{2+} is Mg^{2+}, Ca^{2+}, Sr^{2+}, and Ba^{2+} **[34-37]**. Under circumneutral to slightly alkaline pH conditions (pH 6 to 9) and in a groundwater composition representative of that seen in the 300 Area **[2]**, U(VI) aqueous speciation is dominated by complexes with carbonate, especially ternary complexes that also contain Ca^{2+} or Mg^{2+}. In a similar system with added phosphate, carbonate complexation is still dominant above pH 7.5, but complexation by phosphate dominates below this pH.

Phosphate also affects the solubility of U(VI) in these systems, with uranyl orthophosphate $[(UO_2)_3(PO_4)_2 \cdot 4H_2O]$ and a range of autunite group minerals (**Table 1**) being the most thermodynamically stable phases observed under ambient conditions **[30,32,33,38]**. The predicted stability field for each of these phases has a complex dependence on pH, P_{CO2}, electrolyte cation type and concentration, and phosphate concentration; a thorough description is beyond the scope of this review. *A general conclusion is that uranyl phosphates have predicted solubilities lower than all other common U(VI) phases in groundwater* As an example, in a NaCl electrolyte equilibrated with atmospheric CO_2, U(VI) solubility is greatly reduced in the presence of phosphate, with a minimum solubility a factor of 30 less than the drinking water standard of 30 μg/L (**Fig. 3**). This minimum occurs in the pH range of Hanford 300 Area groundwater (see Section III.A.).

Table 1. *Relevant autunites and meta-autunites*

Mineral/Compound	Formula
Autunite	$Ca(UO_2)_2(PO_4)_2 \cdot 11H_2O$
Meta-Autunite	$Ca(UO_2)_2(PO_4)_2 \cdot 6H_2O$
Chernikovite	$H_3O(UO_2)(PO_4) \cdot 3H_2O$
Sodium Meta-Autunite	$Na(UO_2)(PO_4) \cdot 3H_2O$
Saleeite	$Mg(UO_2)_2(PO_4)_2 \cdot 12H_2O$
Metasaleeite	$Mg(UO_2)_2(PO_4)_2 \cdot 8H_2O$
Torbernite	$Cu(UO_2)_2(PO_4)_2 \cdot 12H_2O$
Metatorbernite	$Cu(UO_2)_2(PO_4)_2 \cdot 8H_2O$
Meta-Ankoleite	$K(UO_2)(PO_4) \cdot 3H_2O$

The specific uranyl phosphate solid that forms in an aqueous system may not necessarily be the thermodynamically most stable phase. Chernikovite, an autunite group mineral, is often described as precipitating under conditions where uranyl orthophosphate is expected to form, and chernikovite transorms to uranyl orthophosphate after boiling, digestion in water, or washing in a solvent **[38-40]**. Chernikovite has been identified at the Shinkolobwe mine, and has been suggested to be a precursor to later-formed uranyl phosphates **[41]**. Chernikovite may be a short-lived but important intermediate phase in the formation of uranyl phosphates **[6]**.

Autunite group minerals can transform between one another through cation exchange reactions **[42-46]**. This class of minerals contains the same major structural unit, the autunite-type sheet, comprised of square bipyramidal uranyl polyhedra linked by
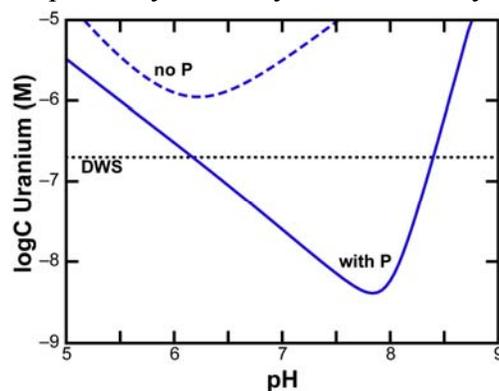

Figure 3. *Uranium(VI) solubility in the absence (dashed) and presence (solid) of 3 mmol/L phosphate in a NaCl electrolyte in equilibrium with atmospheric CO_2. The drinking water standard of 30 μg/L is also shown (dotted).*

phosphate tetrahedra [47-51]. These sheets are linked through interlayer water and charge-balancing cations, analogous to a silicate clay or mica, suggesting a clear mechanism for transformation via cation exchange. Autunite minerals can also partially dehydrate to meta-autunite minerals (e.g., torbernite $[Cu(UO_2)_2(PO_4)_2 \cdot 12H_2O]$ dehydrates to metatorbernite $[Cu(UO_2)_2(PO_4)_2 \cdot 8H_2O]$). This transformation often occurs when autunite minerals are exposed to the atmosphere. Some meta-autunites, like chernikovite, do not have an autunite counterpart, and are likely the stable phase in the presence of water.

Transformation of autunites (or meta-autunites) to uranyl orthophosphate must occur through a dissolution and reprecipitation mechanism, as uranyl orthophosphate has a markedly different structure from that of autunites. The uranyl phosphate structure is comprised of a uranophane-type sheet made of chains of uranyl pentagonal bipyramids linked by phosphate tetrahedra; these sheets are linked by uranyl pentagonal bipyramids bound to the unbonded O atoms of the phosphate groups, resulting in a framework structure [52]. The formation of an autunite as a precursor to uranyl orthophosphate formation suggests that there are mechanistic controls that favor the nucleation and precipitation of autunite-type sheets over other uranyl phosphate structural units. *Knowledge of the mechanisms that determine which uranyl phosphate solids precipitate is critical because metastable phases may form that have different solubilities or dissolution rates than the solids predicted by thermodynamic equilibrium.*

D. Adsorption/Desorption and Precipitation/Dissolution in UO_2^{2+}-PO_4^{3-}-CO_3^{2-} Systems

The concentration of uranium in environmental aquatic systems is primarily controlled by adsorption/desorption and precipitation/dissolution reactions. In carbonate-bearing systems, U(VI) typically displays an adsorption edge at pH 4-5 [53]. Adsorption becomes unfavorable above pH 8-9 because of aqueous complexation of U(VI) by carbonate [53]. Phosphate increases uranium adsorption at low pH, presumably through the formation of ternary surface complexes [54-57]. The presence of phosphate has been shown to enhance adsorption and limit transport of uranium in goethite-coated sand [58]. We are unaware of any studies that have investigated the effects of phosphate on U(VI) desorption processes or rates, although Cheng et al. [58] noted that phosphate causes either irreversible sorption or kinetically slow desorption of U(VI) during transport through goethite-coated sand.

Uranium in phosphate-bearing environmental systems may also form precipitates. We have recently observed rapid uranyl phosphate precipitation in the presence of goethite at mild degrees of supersaturation, including conditions under which adsorption was expected to have caused the initially supersaturated aqueous phase to become undersaturated with respect to known uranyl phosphates [59]. Fuller et al. [25] observed that uranium reaction with apatite $[Ca_5(PO_4)_3OH]$ leads to adsorption and to precipitation as chernikovite and autunite. A similar observation was made in the presence of bone charcoal and bone meal apatite [60]. Murakami et al. [61] observed the formation of nanocrystalline uranyl phosphates downgradient of the Koongarra ore deposit in Australia that were associated with iron oxides. They hypothesized that these formed by adsorption of the many constituent ions onto ferrihydrite followed by precipitation during ferrihydrite recrystallization into goethite or hematite. As noted above, uranyl phosphates have also been found in contaminated soils and sediments at a number of DOE facilities [3,4,10-14]. *Despite these observations, the transition in U(VI) immobilization mechanisms from adsorption to precipitation is still unclear.* We are unaware of systematic studies of the rates of uranyl phosphate precipitation in homogeneous or heterogeneous systems. However, column studies designed to test the feasibility of polyphosphate injection as a

treatment method did indicate that autunite solids formed [5], suggesting that uranyl phosphate precipitation is sufficiently fast to be an effective sequestration mechanism.

Uranyl phosphate dissolution processes and rates were recently investigated. Sowder et al. [62] observed that the uranyl phosphates meta-autunite [Ca(UO$_2$)$_2$(PO$_4$)$_2$·6H$_2$O] and chernikovite dissolved more slowly than uranyl oxyhydroxide phases. Our recent measurements of meta-autunite and sodium meta-autunite [NaUO$_2$PO$_4$·3H$_2$O] dissolution revealed that dissolution is non-stoichiometric, with substantially less uranium released than phosphate [15,16]. Uranyl orthophosphate was identified as a possible product under acidic conditions [15], but the identity of the residual solid phase under neutral to basic conditions is currently unknown [16]. Rates of uranyl phosphate dissolution may increase in vadose zone sediments, as wetting-drying cycles increase swelling and cracking of uranyl minerals, resulting in an increase in the reactive surface area of the minerals [63]. This effect has been seen in arid and semiarid environments, where uranium phases have displayed accelerated rates of corrosion [41,64].

While the molecular mechanisms of uranyl phosphate dissolution are generally unknown, the behavior of related systems can serve to highlight processes that may be important. The dissolution mechanisms of uranyl oxyhydroxides have recently been investigated by Schindler et al. [65-68]. *These mechanisms varied with pH and type of electrolyte cation present.* Under acidic and circumneutral conditions, dissolution occurred primarily through etch-pit formation and growth. The symmetry and elongation direction of the etch pits varied with the concentration and identity of the electrolyte cation. This variation was suggested to be related to the adsorption of electrolyte cations at specific surface sites, altering the dissolution rate along specific crystallographic directions. Cations most similar in size to the dominant cation in the mineral structure had the largest effect on dissolution mechanisms. Hillocks were observed to form under basic conditions, although it was unclear if these were the result of swelling of the structure or precipitation of a secondary phase.

IV. RESEARCH APPROACH

A. Major Hypotheses

The proposed research is designed to test the following major hypotheses. More detailed, task-specific hypotheses are *highlighted* in the project descriptions discussed below.

1. Molecular interactions in solution and at mineral surfaces control the phases that form in systems supersaturated with respect to uranyl phosphate solids.

2. These molecular-scale interactions and the degree of water saturation govern the spatial distribution and precipitation rates of uranyl phosphates in heterogeneous porous media.

3. The solution composition will control uranyl phosphate dissolution rates as a result of molecular-scale factors that govern variations in dissolution mechanisms and the formation of secondary solid phases.

4. Rates of uranyl phosphate dissolution and secondary phase formation can be used to predict the net release rate of U(VI) from phosphate-treated heterogeneous porous media.

5. As result of wetting-drying cycles and increased reactive surface area, the formation of secondary phases and the net rate of U(VI) release will be accelerated under water-unsaturated conditions.

B. General Research Strategy

Our team will test these hypotheses through a research approach that progresses from the molecular-scale to the sediment-scale in two integrated modules (**Fig. 4**). In both modules, the approach will (a) apply techniques to gain molecular-scale insights into reaction mechanisms, (b) quantify rates and mechanisms of processes in controlled laboratory systems, and (c) assess the role of these processes in controlling uranium fate and transport in Hanford sediments. These measurements will be integrated to form a coherent and self-consistent picture of the processes through which phosphate affects the fate and transport of uranium in the environment. Ultimately this approach will be used to develop a conceptual model for the impacts of phosphate on uranium fate and transport in subsurface environments. The two modules are divided into tasks designed to test specific hypotheses. The progression of tasks in each module will build up our knowledge base from the molecular-scale to the sediment-scale. Detailed scientific motivation, the experimental approach, major analytical methods to be used, and the team member(s) responsible for each task are described below.
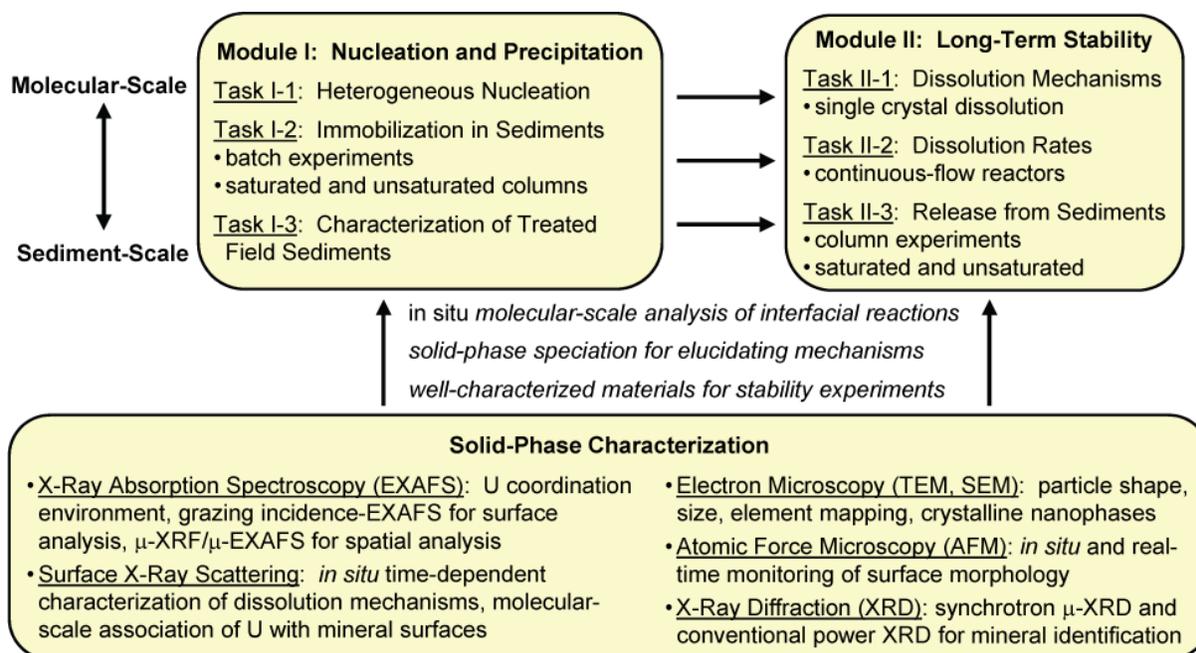

Figure 4. *Research approach to integrate the investigation of mechanisms of uranyl phosphate precipitation and dissolution with the long-term fate of uranium. Two integrated modules combine laboratory-scale experiments with advanced techniques for solid-phase characterization.*

C. Module I – Uranyl Phosphate Nucleation and Precipitation

This module seeks to understand the processes controlling the nucleation and precipitation of uranyl phosphate solids in heterogeneous systems. The results of fundamental studies will be used to interpret processes occurring in Hanford sediments and to develop a reaction-based conceptual model of uranyl phosphate formation in heterogeneous porous media. This conceptual model will be tested by comparing the speciation and distribution of uranium in pristine sediments reacted with model solutions in the laboratory to that in sediments retrieved from the polyphosphate treatment test site.

ii. Task I-1: Mineral-surface controls on uranyl phosphate formation.

Environmental systems contain numerous pre-existing solid phases that can affect precipitation processes. Mineral surfaces can serve as nucleation sites, increasing the rates of precipitation by removing the initial energetic barrier to nucleation in homogenous solution [69]. Consequently, heterogeneous nucleation of uranyl phosphates could lead to precipitation under conditions where these phases are less supersaturated than is required for homogeneous nucleation. Mineral surfaces can also act as templates for mineral growth, leading to oriented growth of a surface precipitate [70], often with a different morphology than would form in homogeneous solution [71]. As adsorption processes may vary with solution conditions, different heterogeneous nucleation mechanisms may operate in different chemical regimes. Understanding these regimes is required for creating a conceptual model of uranyl phosphate formation in the environment.

The Hanford 300 Area subsurface sediments are comprised primarily of silicate minerals, such as feldspars and phyllosilicate clays [2], that provide surfaces for the heterogeneous nucleation of uranyl phosphates. *We hypothesize that mineral surfaces play an active role in uranyl phosphate nucleation and precipitation and that the processes involved vary with solution composition. This variation reflects changes in the molecular-scale mechanisms of nucleation.* We propose to examine heterogeneous nucleation of uranyl phosphates on mineral surfaces as a function of saturation state and solution composition in order to delineate chemical regimes where specific processes operate. These studies will investigate precipitation on single crystal surfaces of select model minerals. Single crystal surfaces are ideal for fundamental studies of nucleation processes as they allow for detailed characterization using in situ microscopic, spectroscopic, and diffraction methods. In situ measurements are needed to resolve the key mechanisms involved in the formation of uranyl phosphates at mineral surfaces. We have selected orthoclase [$KAlSi_3O_8$] (001), muscovite [$KAl_2(AlSi_3)O_{10}(OH)_2$] (001), and alumina [$\alpha$-$Al_2O_3$] (110) for these measurements as they serve as model surfaces of key components in the Hanford subsurface.

Orthoclase was selected as a model feldspar because high-quality single crystals are readily available and the molecular scale structure of this surface in aqueous solution has previously been characterized [72,73]. Although albite [$NaAlSi_3O_8$] is more common in Hanford sediments [74], orthoclase is an acceptable substitute as both surfaces are expected to lose their cation (K^+/Na^+) to solution, effectively presenting identical surfaces upon which nucleation may occur. Muscovite (001) was selected to serve as a model for basal planes of phyllosilicates, including interlayers of clay minerals. Its surface has been well-studied [75-77] and samples are readily available. The alumina (110) surface serves as a model for the edges of phyllosilicates, which are important adsorption sites for uranium under circumneutral pH conditions, including in the 300 Area vadose zone [4,78-82]. Alumina (110) has similar aluminol surface functional groups to exposed octahedral sheets at the edges of phyllosilicate clays and this surface has been characterized [83].

The heterogeneous nucleation of uranyl phosphates on these surfaces will be examined as a function of pH, phosphate and U(VI) concentration, and the type and concentration of other groundwater cations (Na^+, Ca^{2+}). All experiments will be performed in solutions equilibrated with atmospheric CO_2. Initial measurements will involve reaction of crystal substrates in batch solutions; surface products will be characterized ex situ by scanning electron microscopy with energy dispersive spectrometry (SEM-EDS) and atomic force microscopy (AFM). We will specifically examine whether nucleation processes differ on the surfaces of different minerals

9

and on individual minerals under varying chemical conditions. Once chemical regimes have been delineated through this initial survey, select representative systems will be further explored through in situ studies. In situ AFM measurements of nucleation and growth on specific surfaces will provide insight into the nanoscale mechanisms and rates of uranyl phosphate precipitation. Grazing-incidence extended X-ray absorption fine structure (EXAFS) measurements will be conducted to characterize the initial precipitation products, distinguishing between different structural classes of uranyl phosphate precipitates (e.g., autunites versus uranyl orthophosphate). X-ray reflectivity measurements will be used to explore whether precipitation is epitaxial, and surface powder XRD will be used to determine the identity and crystallinity of the mineral phases that precipitate. Catalano will lead this task.

iii. Task I-2: Uranyl phosphate precipitation in pristine Hanford sediments.

Precipitation of uranyl phosphates in heterogeneous porous media, such as Hanford sediments, may occur through homogeneous nucleation from solution and/or heterogeneous nucleation on mineral surfaces (as in Task I-1). *We hypothesize that uranyl phosphate precipitation will be facilitated by the presence of sediments and will be accelerated by wetting-drying cycles under water-unsaturated conditions.* We will examine the geochemical factors controlling the precipitation, location, and identity of uranyl phosphate solids in Hanford sediments using both batch and column experiments. Batch experiments will be conducted with and without uncontaminated Hanford sediments over a wide range of solution compositions. Based on the results of the batch experiments, selected solution compositions will be selected for use in column experiments. Column experiments will be performed under both water-saturated and water-unsaturated conditions. Unsaturated conditions are particularly relevant to uranyl phosphate formation at the Hanford 300 Area because of planned pilot testing of the polyphosphate treatment method (see Section III.B.). Together these experiments will provide the dataset needed to develop a reaction-based conceptual model for uranyl phosphate formation processes in sediments. Such a model is needed to describe and predict processes that occur in subsurface systems at DOE sites. Giammar will lead this task; Wellman will conduct unsaturated column experiments and Catalano will assist in product characterization.

Batch Experiments. The extent of solution supersaturation necessary for precipitation will be investigated by conducting experiments at low and high degrees of supersaturation with respect to the uranyl phosphate minerals of interest. The degree of supersaturation is expressed as the saturation index for a specific solid phase based on the initial solution composition. The saturation index of autunite, for example, is given in equation 1.

The effect of solution composition on uranyl phosphate precipitation will be examined by conducting experiments at varying pH, source of phosphate, concentrations of phosphate and uranium(VI), and the concentrations of other

$$SI = \log \frac{\{Ca^{2+}\}\{UO_2^{2+}\}^2\{PO_4^{3-}\}^2}{K_{sp}} \qquad (1)$$

groundwater cations (Na^+, Ca^{2+}). Specific combinations of these parameters will yield compositions that are predicted to be supersaturated with respect to different uranyl phosphate phases. These phases include autunite [$Ca(UO_2)_2(PO_4)_2 \cdot 11H_2O$], sodium meta-autunite [$Na(UO_2)(PO_4) \cdot 3H_2O$], chernikovite [$H_3O(UO_2)(PO_4) \cdot 3H_2O$], and uranyl orthophosphate [$(UO_2)_3(PO_4)_2 \cdot 4H_2O$]. Depending on the kinetics and mechanisms of nucleation and growth, the most thermodynamically favorable phase may not actually form and a metastable solid phase

may be dominant. A broad range of aqueous compositions will be examined to encompass the conditions of a variety of uranium-contaminated sites; within this range, specific conditions will emulate the groundwater chemistry of the Hanford 300 Area. Experiments will investigate the pH range of 5-9. Phosphate will be added in one of three forms: sodium orthophosphate, the polyphosphate compound sodium tripolyphosphate, and the mixture of orthophosphate, pyrophosphate, and tripolyphosphate that is used in the pilot-scale treatment test at the Hanford 300 Area. The active species in promoting precipitation is orthophosphate; however, polyphosphates provide a slow release of orthophosphate as they undergo hydrolysis, which can have advantages when used in remediation [5]. In groundwater at most relevant sites, notably the Hanford 300 Area, Na^+ and Ca^{2+} are the dominant cations [2] and are expected to make autunite and/or sodium meta-autunite the most stable uranyl phosphate minerals. The concurrent addition of Na^+ when adding a source of phosphate may lead to systems where sodium meta-autunite is the dominant phase [5].

The effect of mineral surfaces on uranyl phosphate precipitation will be examined by comparing the results of experiments with sediments with those from sediment-free control experiments. Pristine, uncontaminated sediments from the Hanford IFC (located in the 300 Area) will be used in these studies. Sediment materials will be supplied from the Hanford IFC (see attached letter from Mark Freshley). As uranium has been shown to not associate with particles larger than 2 mm in the 300 Area vadose zone [2], only the <2 mm size fraction will be used for study. The sediments may enhance precipitation by providing surfaces for the nucleation of uranyl phosphate precipitates, as investigated in Task I-1. However, the presence of the sediments may also inhibit precipitation by adsorbing U(VI) and/or phosphate, which can result in lower dissolved concentrations and consequently lower degrees of supersaturation; we have observed such an effect for the co-adsorption of lead or uranium with phosphate on goethite-coated sand [59,84]. Selected uranium-free and phosphate-free solutions will be used to establish the equilibrium adsorption of U(VI) and phosphate to the sediments over the range of pH values studied.

Batch experiments will use a low solid:water ratio (10-100 g/L) relative to that used in column experiments (~12,000 g/L), which allows the batch suspensions to be continuously-mixed in flasks on a rotary shaker. Sediments will first be pre-equilibrated with an aqueous solution at the desired pH and containing all constituents other than the uranium and phosphate source. All experiments will be performed in solutions equilibrated with atmospheric CO_2. After the pre-equilibration period, uranium and the phosphate source will be added to the suspensions. At regular intervals for up to one week, samples of the suspension will be filtered and preserved for analysis. Concentrations of U, Ca, Na, and P will be determined by inductively coupled plasma mass spectrometry (ICP-MS). The concentration of free orthophosphate will be determined by a colorimetric method. The aqueous composition will be used to calculate the saturation index of the solution with respect to the various uranyl phosphate solids that may have precipitated. Calculations will be performed using equilibrium speciation software [85,86] and equilibrium constants from the latest critically-reviewed databases and peer-reviewed publications [30-33,37]. The formation of apatite $[Ca_5(PO_4)_3OH]$ will be thermodynamically favorable in some of the initial solutions; however, apatite has not been observed when reacting Hanford groundwater with polyphosphate because the native calcium concentration remains at relatively low levels [5]. Further, apatite has not been observed at most subsurface sites where uranyl phosphates have been found [3,10-13]. Although apatite formation is not expected in most experiments, its saturation index will be considered in

interpreting aqueous composition results and solid phase analyses will probe for apatite formation.

The identity and spatial distribution of uranyl phosphate phases will be determined by analyzing uranium-loaded sediments collected at the conclusion of the batch experiments. The uranyl phosphates that precipitated in sediment-free control experiments will also be characterized. The spatial distribution of uranium in the sediments and the morphology of uranyl phosphate precipitates will be examined by SEM-EDS and transmission electron microscopy (TEM). Precipitated solid-phases will be characterized using EXAFS spectroscopy, synchrotron X-ray diffraction, and μ-EXAFS/μ-XRD measurements to develop a mechanistic understanding of the formation and identity of the resulting uranium phase(s) as a function of solution composition. Pure U(VI)-containing phases isolated from the batch reactors will also be analyzed by X-ray diffraction (XRD). Details of these methods are presented in Section IV.E.

Column Experiments. Series of saturated and unsaturated column tests will be conducted as a function of the solution composition for a subset of conditions determined from the results of the batch experiments. Columns will be packed with uncontaminated Hanford sediments and saturated with uncontaminated synthetic groundwater to start each experiment. The sediments in the columns will have an effective porosity (19%) and bulk density (2.2 g/cm^3) similar to that of the Hanford 300 Area aquifer. Following the attainment of hydraulic and chemical equilibrium, the influent solutions will be changed to uranium-spiked and phosphate-amended synthetic groundwater. The columns will first be loaded with uranium from a uranium-spiked synthetic groundwater, and they will then be treated with uranium-free synthetic groundwater that contains orthophosphate or polyphosphate. This method will simulate the formation of uranyl phosphates during the treatment of uranium-contaminated sediments by phosphate addition. In addition to precipitating as uranyl phosphates, U(VI) and phosphate can also adsorb to solid phases; as has been observed with iron oxides [54,58], phosphate may enhance U(VI) adsorption through the formation of ternary U(VI)-phosphate-mineral surface complexes. The results of the batch experiments at undersaturated conditions will be used to determine the expected degree of U(VI) and phosphate adsorption. The influent solutions to columns can then be designed to promote uranyl phosphate precipitation while still accounting for the influence of adsorption.

For each condition, duplicate columns will be used. After being loaded with uranyl phosphates, the first column will be used for analysis of the speciation and spatial distribution of uranyl phosphates by the same techniques just described for batch experiments. The second column will be saved and used for the dissolution experiments of Task II-3.

Water-saturated columns ($r = 1.25$ cm, $L = 15$ cm) will be operated in an upflow mode, which helps maintain water saturation over the course of the experiment. A peristaltic pump will provide an influent flow rate corresponding to an advective velocity of 1 m/d. The effluent from the columns will be collected at regular intervals by fraction collectors and the dissolved concentrations of U, Ca, Na, total phosphate, and orthophosphate will be measured.

Column experiments at water-unsaturated conditions will be performed using the pressurized unsaturated flow (PUF) system (**Fig. 5**) [87-90]. The PUF system allows controlled dynamic changes in water content that simulate the periodic wet-dry cycling experienced in the vadose zone and capillary fringe. The columns will be saturated with Hanford groundwater and then pressurized and drained to the desired water content. This process of fully saturating and reducing the water content to the desired level minimizes preferential flow paths and hysteresis and achieves the most consistent, uniform attainment of water content within a series of

12

unsaturated columns. Slight changes in pH, conductivity, and water content that occur during dissolution and precipitation reactions are continuously logged via the PUF system; as such, the PUF system is ideally suited to conducting unsaturated weathering and precipitation experiments **[89,91,92]**. The PUF system **[87,88]**, which is similar to a Wierenga column, consists of a polyetheretherketone column ($r = 0.96$ cm, $L = 7.62$ cm) with a porous titanium plate; the plate has a nominal pore size of 0.2 μm and is sealed in the bottom of the column. Once the porous titanium plate is water saturated,

Figure 5. *PUF system for unsaturated column experiments with Hanford sediments.*

water, but not air, is allowed to flow through the 0.2-μm pores, as long as the applied pressure differential does not exceed the air entry relief pressure, referred to as the bubble pressure of the Ti-plate. If the pressure differential is exceeded, air will escape through the plate and compromise the capability to maintain unsaturated flow conditions in the column **[87,88]**.
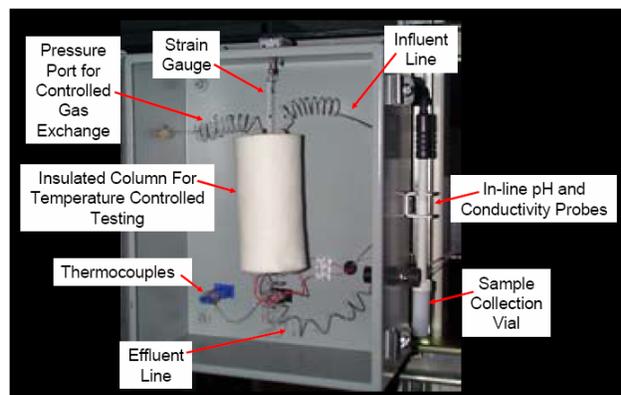
iv. Task I-3: Characterization of uranium speciation in sediments from field testing of polyphosphate injection.

The analysis of sediments from the site of the polyphosphate injection test site by advanced characterization techniques in this project will complement on-going activities in projects funded by EM. As described in Section III.B., testing is underway to evaluate the ability of polyphosphate injections into U-contaminated sediments at the Hanford site to reduce groundwater uranium concentrations and stabilize uranium in a solid phase in the saturated zone, capillary fringe, and vadose zone. The EM-funded projects will do basic characterization of the testing site, including long-term monitoring of groundwater cation and anion concentrations. Additionally, limited analyses will be conducted on post-test borehole core sediments. XRF, XRD and SEM will be used to conduct a survey of uranium phases present; selective extractions will be conducted to discern the geochemical environment in which uranium is associated. Detailed measurements of uranium speciation and distribution in treated sediments will not be determined under the EM project because of budget constraints. However, evaluation of the post-injection long-term stability of uranium in the vadose zone, capillary fringe, and saturated zone requires this information. *We hypothesize that the identity and spatial distribution of uranyl phosphates in these sediments will be unique to the hydrogeochemical environment in which they formed and can be correlated to the groundwater composition and the mineral surfaces available for heterogeneous nucleation.* We will characterize the speciation and distribution of uranium in sediment samples taken from the treatment zone to identify the process(es) responsible for reduction in uranium groundwater concentrations and to test the reaction-based conceptual model we will develop in Task I-2.

μ-XRF measurements of select, representative samples will be used to image the distribution of uranium with ~1 ppm sensitivity **[93]**, and areas with elevated uranium concentrations will be characterized by μ-EXAFS spectroscopy and μ-XRD. For samples with total solid-phase uranium concentrations >100 ppm (the effective detection limit of U EXAFS),

bulk EXAFS measurements will be used to quantify the distribution of uranium among different species identified using X-ray microbeam methods (additional details are provided in Section IV.E.). Catalano will lead this task with assistance from Wellman.

D. Module II – Long-Term Stability of Uranyl Phosphates

This module seeks to understand the processes that control the long-term stability of uranyl phosphate solids in subsurface environments. We will characterize the nanoscale mechanisms and products of dissolution and connect these to macroscopic dissolution rates. These studies will be used to understand dissolution rates and processes observed in laboratory-reacted Hanford sediments at water-saturated and unsaturated conditions.

i. Task II-1: Dependence of uranyl phosphate dissolution mechanisms and products on solution composition.

The stability of uranyl phosphate precipitates and the resulting impact on groundwater uranium concentrations depends on the mechanisms and rates of dissolution of these phases. Dissolution mechanisms may depend on solution composition (pH, concentration of cations and anions, etc.), and different mechanisms may control the rate of uranium release under different chemical regimes. *We hypothesize that dissolution mechanisms operating at the mineral-water interface vary with solution composition.* We will investigate the dissolution mechanisms of uranyl phosphates and relate the variation of these mechanisms to pH and the identity and concentration of cations present.

In this task microscopy and X-ray scattering methods will be used to investigate the dissolution mechanisms of uranyl phosphates. Single crystals of autunite [$Ca(UO_2)_2(PO_4)_2 \cdot 11H_2O$] and sodium meta-autunite [$Na(UO_2)(PO_4) \cdot 3H_2O$] will be synthesized using previously described procedures [47,49]. These phases have been chosen because their macroscopic dissolution behavior has been studied in the past [15,16] and they are the phases most likely to form in the Hanford subsurface during polyphosphate treatment.

The effects of pH and groundwater composition, specifically the type and concentration of electrolyte cations, on the nanoscale dissolution mechanism of autunite and sodium meta-autunite crystals will be explored. All solutions will be equilibrated with atmospheric CO_2. Initial measurement will investigate a wide range of conditions. Nanoscale surface features after reaction, such as etch pits or surface precipitates, will be compared to features on fresh surfaces using ex situ AFM measurements. Once a range of conditions have been studied and mechanistic regimes delineated, in situ AFM measurements will be made in select, representative solutions to observe dissolution processes in real time. For select conditions, in situ time-dependent X-ray reflectivity measurements will be made to examine the rates and mechanisms of dissolution reactions at the molecular-scale, analogous to what has been done for feldspar surfaces [94]. These experiments will determine the dissolution rates of specific surfaces of uranyl phosphates and whether dissolution on these surfaces occurs at step sites, terrace sites, or both. The observed results will be used to delineate mechanistic regimes that likely correlate with variations in macroscopic dissolution rates. This type of information has been obtained in past studies of feldspar dissolution using similar methods [94,95]. Catalano will lead this task.

14

ii. Task II-2: Macroscale uranyl phosphate dissolution rates and their connection to nanoscale dissolution behavior.

In sediments containing uranyl phosphates, dissolution rates will be a primary control on uranium concentrations in groundwater. Quantification of these rates and their dependence on groundwater composition is needed to predict the long-term stability of uranyl phosphate minerals in subsurface environments. *We hypothesize that the dissolution rates of uranyl phosphate minerals are functions of the solution composition that can be quantified using general dissolution rate equations.* The dissolution rates of pure forms of uranyl phosphate minerals will be determined as a function of solution composition. For select conditions, experiments will also probe the rates of transformation of one solid phase into a different solid phase; for example, autunite may be transformed into sodium meta-autunite when it is contacted with high concentrations of dissolved Na^+. Experiments will initially focus on autunite and sodium meta-autunite in order to examine rate differences between these two related mineral phases. We will also examine meta-autunite $[Ca(UO_2)_2(PO_4)_2 \cdot 6H_2O]$, as this partial dehydration product of autunite may form under unsaturated conditions and display different dissolution behavior. Depending upon the specific phases observed in Tasks I-2 and I-3, the dissolution rates of chernikovite and uranyl orthophosphate may also be investigated. Each solid will be synthesized in its pure form following published methods [47,49,52,96]. The identity and purity of each phase will be confirmed by X-ray diffraction and complete digestion prior to use in dissolution experiments.
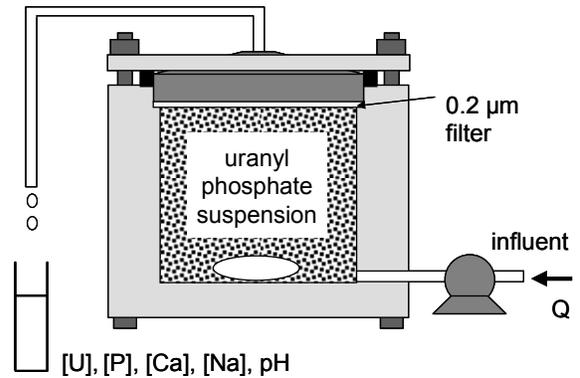

Figure 6. Flow-through reactor for rates.

Custom-built flow-through reactors (**Fig. 6**) will be used to quantify the dissolution and transformation rates as a function of pH and solution composition. Because reaction products are continuously flushed from the reactors, reaction rates are not affected by the accumulation of products as can occur in batch reactors. Flow-through reactors also avoid transient effects associated with reactor start-up or the introduction of reactants from concentrated stock solutions. We have previously used this method to quantify the dissolution rates of oxyhydroxide, silicate, and phosphate minerals [84,97,98]. The proposed work builds upon our previous studies of autunite and sodium meta-autunite dissolution [15,16], which were done using similar flow-through reactors, by examining the rates over a broader range of solution compositions and directly characterizing the residual solid phases.

Dissolution rates ($mol/m^2/h$) are quantified from the establishment of steady-state dissolution using equation 2, in which C_{inf} and C_{eff} are the influent and effluent concentrations of uranium or phosphate (mol/L), t_{res} is the hydraulic residence time of the reactor (h), [solids] is the concentration of the suspension (g/L), and A is the specific surface area of the solid (m^2/g). Influents to the reactors will be fixed at the desired pH and solution composition, and the effluent will be periodically monitored for pH and dissolved U, P,

$$Rate = \frac{(C_{eff} - C_{inf})}{t_{res} \cdot [solids] \cdot A} \quad (2)$$

$$Rate = k_0 \cdot \{H^+\}^{n_{H^+}} \cdot \left(1 - e^{\frac{\Delta G_r}{RT}}\right) \quad (3)$$

$$\Delta G_r = RT \ln \frac{\{Ca^{2+}\}\{UO_2^{2+}\}^2 \{PO_4^{3-}\}^2}{K_{sp}} \quad (4)$$

15

Ca, and Na. For a given temperature, the dissolution rate is affected by the solution pH (role of $\{H^+\}$), the overall thermodynamic driving force for the reaction (ΔG_r), and an intrinsic rate constant k_0 (mol/m^2/h) specific to the material [99,100] (equation 3). Recent research on the dissolution rate of the sodium uranyl silicate mineral Na-boltwoodite used a similar rate equation and included a term for rate enhancement by dissolved inorganic carbon [101,102]. The thermodynamic driving force is included as the free energy of the reaction, which is a function of the solubility product of the solid (K_{sp}) and the composition of the aqueous solution (equation 4). Dissolution rates will be measured over the pH range from 4-8 to determine the value of n_{H+}. All influent solutions will be equilibrated with atmospheric CO_2.

While most experiments will use influent solutions that contain ultrapure water buffered at the desired pH, additional experiments will include phosphate and groundwater cations to probe their effects on the dissolution rate. The inclusion of phosphate in the influent will lower the thermodynamic driving force for dissolution and should result in lower overall dissolution rates. The inclusion of Ca and Na in the influent will be used to examine the rates of transformation of one uranyl phosphate solid into another. The ratios of Ca and Na to U and P in the effluent can provide insight into whether the reactions occur by dissolution of one phase followed by precipitation of a secondary phase or by direct solid phase transformation.

The solids will be collected at the conclusion of the flow-through experiments to characterize changes in the composition of the solid phase and to investigate the formation of secondary phases. Uranyl phosphate dissolution is often non-stoichiometric, with release of phosphate in excess of uranium [15,16]. The remaining solids will be enriched in uranium; identification of potential secondary phases, such as uranyl orthophosphate or schoepite $[(UO_2)_8O_2(OH)_{12}\cdot12H_2O]$, will be critical to establishing the long-term controls on uranium concentrations that result from uranyl phosphate dissolution. Giammar will lead this task.

iii. Task II-3: Uranyl phosphate dissolution rates in reacted Hanford sediments under saturated and unsaturated conditions.

Dissolution rates measured for single minerals in batch experiments will provide fundamental constraints on the release rates in more complex heterogeneous porous media. In addition, studies of the mechanisms of dissolution will highlight the chemical regimes where specific processes dominate as well as potential secondary phases that may form in uranyl phosphate-bearing sediments. The added complexity of porous media may alter the rates of dissolution, and the variable saturation state of sediments in the vadose zone and capillary fringe may lead to changes in dissolution processes. *We hypothesize that uranyl phosphates will display similar dissolution behavior and secondary products in Hanford sediments as in homogeneous systems, but that uranium release will be retarded by adsorption reactions. We further hypothesize that the wetting-drying cycles at water-unsaturated conditions will accelerate the formation of secondary products and increase dissolution rates as a result of increased reactive surface area of uranyl phosphate minerals after dehydration.* The dissolution rates of uranyl phosphate minerals in Hanford sediments will be measured by using columns of sediments that were treated with uranium and phosphate in Task I-2. The spatial distribution and identity of uranyl phosphates will have been fully characterized in one column for each loading condition in Task I-2, and the duplicate column is available for the dissolution experiments of this task. Columns selected for use in this task will include ones that contain a single uranyl phosphate mineral as well as ones that contain mixtures of different minerals. The columns with

a single uranyl phosphate phase will be particularly valuable in establishing the relationship of the fundamental dissolution rate equations determined in Task II-2 to the macroscopic release of uranium from sediments subjected to advective flow.

Saturated and unsaturated column studies will be performed by the same methods described in Task I-2 for uranyl phosphate formation in sediment-packed columns. Water saturated columns will be run in an upflow mode with flow rates that provide flow velocities of 0.2 to 2 m/d. Columns at unsaturated conditions will use the pressurized unsaturated flow (PUF) system [87-90] to control the water content and simulate the wetting-drying cycles that can alter the dissolution and transformation of uranyl phosphate precipitates.

In contrast to the experiments performed in Task I-2, these experiments will use uranium-free synthetic groundwater with no added phosphate. Solution compositions will be prepared to simulate uncontaminated Hanford groundwater. The dissolution rates of uranyl phosphates will be investigated by measuring the dissolved concentrations of U, P, Ca, and Na over time. The overall release of these elements is affected by adsorption as well as by dissolution reactions, and the interpretation of elution curves will account for the capacity of the sediments to adsorb the U(VI) and phosphate released during the dissolution of uranyl phosphates. The results of the batch experiments in Task I-2 that focused on equilibrium adsorption will be used to constrain adsorption estimates. If characterization of the sediments in the column during Task I-2 identified apatite precipitation, then release rates of Ca and P will be monitored to estimate the influence of the apatite dissolution rate on the overall release rates of U(VI) and P. At the conclusion of each column-based dissolution experiment, the sediments will be removed and analyzed for their total elemental compositions to verify changes in uranyl phosphate content and composition. Selected sediment samples will be investigated by SEM-EDS to examine the spatial relationships among U, P, and the relevant cations. Based on these distributions, sediments may be further characterized by synchrotron-based μ-XRF, μ-EXAFS, and μ-XRD techniques to identify the specific uranyl phosphate phases present and to examine changes in uranium distribution after reaction.

The measured rates of uranium release from the columns can be affected by both the rates of the relevant chemical reactions and of the hydraulic transport processes. The water-saturated column experiments will be conducted at multiple flow rates to determine the influence of the hydraulic residence time on the extent of uranyl phosphate dissolution. If the overall uranium release rate is controlled by the kinetics of the dissolution reaction, then the effluent uranium concentrations will be strong functions of the flow rate supplied to the columns. However, if the dissolution-precipitation reactions achieve equilibrium on time-scales faster than those of the transport processes, then the effluent uranium concentration will be independent of flow rate. Giammar will lead this task; Wellman will perform the unsaturated column experiments and Catalano will assist with solid-phase characterization

E. Characterization Methods

A number of advanced characterization methods will be used in the proposed work. Methods that go beyond conventional mineralogical characterization are reviewed below.

i. Synchrotron-based X-ray Methods

A number of synchrotron-based X-ray methods will be utilized in the proposed work. EXAFS spectroscopy is an element-specific technique that will provide information on the local

coordination environment of uranium. EXAFS spectra can serve to distinguish between adsorbed and precipitated uranium. For uranium precipitated in uranyl phosphates, the spectra can be used to identify the mineral phases that formed (although it cannot distinguish between the autunites/meta-autunite [103]), including those with limited long-range order that makes identification by conventional X-ray diffraction challenging. Grazing incidence EXAFS is useful for investigating the speciation of an element on a flat solid surface [104]. X-ray reflectivity probes the structure of surfaces and interfaces [105] and is useful for characterizing the relationship of surface precipitates to the underlying mineral surface.

X-ray microprobe methods (μ-XRF, μ-EXAFS, μ-XRD) will be used to determine the spatial variation in U solid-phase concentration and speciation with micrometer resolution. These methods have been applied to the characterization of uranium speciation and distribution in contaminated sediment samples from the Hanford 300 Area [3,4] and beneath tank BX-102 [106,107]. All synchrotron-based techniques will be performed using beamlines at the Advanced Photon Source (APS) at Argonne National Laboratory. Catalano has been using the APS in his research since 2000, and he has been the PI or co-PI on 23 successful APS beamtime proposals.

ii. Atomic Force Microscopy (AFM)

AFM measures the nanoscale topography of a solid surface by rastering a small tip across the surface. This tip is typically a few nm wide, and AFM is sensitive to topographic features having as small as ~1 Å of relief. Imaging can be performed in air or liquid, and sequential images can be taken at rates as fast as 1 per minute under normal operation. AFM has been used extensively to study mineral growth and dissolution process. Relevant examples include imaging the heterogeneous nucleation of lead phosphate on apatite [70,71], surface precipitation of schoepite [$(UO_2)_8O_2(OH)_{12} \cdot 12H_2O$] on calcite [108], and dissolution of the surfaces of uranyl oxyhydroxides [65-68]. All AFM imaging in this proposal will be performed using an Agilent 5500 AFM recently installed in Catalano's laboratory at Washington University.

V. EXPECTED SCIENTIFIC CONTRIBUTIONS

The proposed work will lead to an enhanced understanding of the processes through which uranyl phosphates control uranium fate in contaminated subsurface environments. Key molecular-scale mechanisms involved in uranyl phosphate formation and long-term stability will be characterized, and the effects of these mechanisms on sediment-scale processes will be determined. The proposed work will: (1) Identify the mechanisms through which mineral surfaces induce and control uranyl phosphate precipitation, and the chemical regimes where individual mechanisms are significant; (2) Determine how groundwater composition and water saturation state affects uranyl phosphate formation in heterogeneous porous media; (3) Validate laboratory studies of uranyl phosphate formation processes by characterizing uranium speciation in contaminated sediments treated with polyphosphate in a pilot-scale field test; (4) Characterize the rates and mechanisms of uranyl phosphate dissolution at the nanoscale; (5) Quantify the dependence of macroscopic dissolution rates of uranyl phosphates on groundwater composition and relate the rates to nanoscale processes; and (6) Determine the dissolution rates of uranyl phosphates in heterogeneous porous media under water saturated and unsaturated conditions. These studies will serve as a foundation for the development of a robust conceptual model to describe the effects of phosphate on the environmental fate and transport of U(VI).

VI. RELEVANCE TO ERSD MISSION

The ERSD mission is to "provide (by 2015) sufficient scientific understanding to allow a significant fraction of DOE sites to incorporate coupled biological, chemical and physical processes into decision making for environmental remediation." This proposal seeks to advance the scientific understanding of the processes that control uranyl phosphate fate in subsurface systems. Uranyl phosphates occur frequently in contaminated soils and sediments at DOE sites, and substantial quantities of additional uranyl phosphate solids are expected to form as a result of phosphate-based remediation methods now under pilot testing. The proposed work will provide the scientific basis for credibly predicting the formation and long-term stability of uranyl phosphates in the subsurface at key contaminated DOE sites, most notably at the Hanford 300 Area. This knowledge is necessary for effective application of new remediation strategies that will mitigate the environmental impact of past nuclear activities.

VII. PROJECT MANAGEMENT

A. Project Team

The proposed research is a collaborative effort among Dr. Jeffrey Catalano (PI) and Dr. Daniel Giammar (Co-PI) at Washington University in St. Louis and Dr. Dawn Wellman (Co-PI) at Pacific Northwest National Laboratory. Our interdisciplinary team has complementary expertise in environmental geochemistry and environmental engineering that allows us to explore the effects of phosphate on uranium fate from the molecular-scale to the sediment-scale. Catalano will lead this interdisciplinary team as his research expertise encompasses much of the proposed work. In Catalano's past Hanford-related research, he determined that chromium was partially reduced from Cr(VI) to Cr(III) in the vadose zone beneath tank SX-108 [109] and that uranium precipitated as the uranyl silicate mineral sodium boltwoodite beneath tank BX-102 [106]. In addition, he characterized the uranium speciation in a depth sequence of sediments from the North Processes Ponds of the Hanford 300 Area, noting that uranium speciation changed from being incorporated in calcite in the (now excavated) pond sediments to being adsorbed on phyllosilicates and precipitated as uranyl phosphates in the underlying vadose zone [4]. Catalano has also performed research on fundamental aspects of uranium, arsenic, selenium, and zinc adsorption processes and mechanisms [78,110-114], cobalt coprecipitation and sorption processes in model Hanford sediments and alkaline aluminate solutions [115], and the molecular-scale arrangement and ordering of interfacial water near iron and aluminum oxide surfaces [116,117].

Dr. Giammar has integrated laboratory-based aqueous and solid characterization tools to investigate rates and mechanisms of reactions of heavy metals and radionuclides, including uranium, at mineral surfaces [84,97,98,118-121]. Giammar's expertise in continuously-stirred flow-through reactors coupled with solid and solution phase characterization are essential to Tasks I-2, II-2, and II-3. Dr. Wellman has expertise in studying geochemical processes in natural and engineered systems, and she has worked extensively on phosphate-based remediation processes for in situ immobilization of uranium, including work at the Hanford Site funded by the DOE Office of Environmental Management and the Office of Biological and Environmental Research [5,15,16,20-24,27,122-124]. Wellman will provide materials from the polyphosphate treatment test site and will perform unsaturated column studies for Tasks I-2 and II-3. These unsaturated column studies are the key contribution from Wellman; they are outside the expertise

of the other PIs and require the unique facilities at Pacific Northwest National Laboratory and Wellman's expertise. At Washington University, one postdoctoral scientist and one graduate student from the Department of Earth and Planetary Sciences and one postdoctoral scientist and one graduate student from the Department of Energy, Environmental, and Chemical Engineering will participate in the proposed research. An additional graduate student will work at Pacific Northwest National Laboratory.

B. Management Plan

Catalano will be responsible for overall project management and administration. All of the PIs on this project will be responsible for individual tasks or components of tasks as specified in Section IV. The project team will hold an annual meeting to discuss research plans for the upcoming year. Research results will also be discussed in years 2 and 3. The team will meet at PNNL in Year 1, and at Washington University in Years 2 and 3. During the Year 1 meeting at PNNL, the team will visit the polyphosphate test site and Hanford FRC to gain a better understanding of the primary contaminated sites of relevance to the proposed work. The team will hold quarterly videoconferences to discuss recent results and coordinate research activities. Catalano will maintain frequent contact with all of the co-PIs. Catalano and Giammar will each mentor a postdoctoral scientist and a graduate student, and Wellman will mentor a graduate student.

VIII. PROJECT PERFORMANCE SITE

The proposed activities will take place at Washington University in St. Louis and Pacific Northwest National Laboratory (PNNL). Tasks I-1, II-1, and II-2 will take place at WUSTL. Tasks I-2, I-3, and II-3 will take place at both WUSTL and PNNL.

IX. PROJECT TIMELINE

The proposed work will be executed according to the following project timeline:

	Year 1	Year 2	Year 3
Module I – Uranyl Phosphate Nucleation and Precipitation			
Task I-1: Heterogeneous Nucleation	▬		
Task I-2: Immobilization in Sediments	▬	▬	
Task I-3: Characterization of Treated Field Sediments		▬	
Module II – Long-Term Stability of Uranyl Phosphates			
Task II-1: Dissolution Mechanisms		▬	▬
Task II-2: Dissolution Rates		▬	
Task II-3: Release Rates from Treated Sediments			▬

The project team will adjust this timeline as needed based on the initial results in order to pursue the most important scientific questions relevant to uranyl phosphate formation and stability in subsurface environments.

APPENDIX A: LITERATURE CITED

[1]   Peterson, R. E.; Freeman, E. J.; Murray, C. J.; Thorne, P. D.; Truex, M. J.; Vermeul, V. R.; Williams, M. D.; Yabusaki, S. B.; Zachara, J. M.; Lindberg, J. L.; McDonald, J. P. *Contaminants of Potential Concern in the 300-FF-5 Operable Unit: Expanded Annual Groundwater Report for Fiscal Year 2004*; PNNL-15127; Pacific Northwest National Laboratory: Richland, WA, 2005.

[2]   Zachara, J. M.; Davis, J. A.; McKinley, J. P.; Wellman, D. M.; Liu, C. X.; Qafoku, N. P.; Yabusaki, S. B. *Uranium Geochemistry in Vadose Zone and Aquifer Sediments from the 300 Area Uranium Plume*; PNNL-15121; Pacific Northwest National Laboratory: Richland, WA, 2005.

[3]   Arai, Y.; Marcus, M. K.; Tamura, N.; Davis, J. A.; Zachara, J. M., Spectroscopic evidence for uranium bearing precipitates in vadose zone sediments at the Hanford 300-area site. *Environmental Science & Technology* **2007,** *41*, 4633-4639.

[4]   Catalano, J. G.; McKinley, J. P.; Zachara, J. M.; Heald, S. M.; Smith, S. C.; Brown, G. E., Jr., Changes in uranium speciation through a depth sequence of contaminated Hanford sediments. *Environmental Science & Technology* **2006,** *40*, 2517-2524.

[5]   Wellman, D. M.; Pierce, E. M.; Richards, E. L., In Situ Uranium Stabilization through Polyphosphate Remediation: Development and Demonstration at the Hanford Site 300 Area, Washington State. In *Waste Management Research Trends*, Golush, T. V., Ed. Nova Science Publishers, Inc.: Hauppage, NY, 2008.

[6]   Finch, R.; Murakami, T., Systematics and paragenesis of uranium minerals. *Reviews in Mineralogy* **1999,** *38*, 91-179.

[7]   Wilkins, M. J.; Livens, F. R.; Vaughan, D. J.; Beadle, I.; Lloyd, J. R., The influence of microbial redox cycling on radionuclide mobility in the subsurface at a low-level radioactive waste storage site. *Geobiology* **2007,** *5*, 293-301.

[8]   Wu, W. M.; Carley, J.; Luo, J.; Ginder-Vogel, M. A.; Cardenas, E.; Leigh, M. B.; Hwang, C. C.; Kelly, S. D.; Ruan, C. M.; Wu, L. Y.; Van Nostrand, J.; Gentry, T.; Lowe, K.; Mehlhorn, T.; Carroll, S.; Luo, W. S.; Fields, M. W.; Gu, B. H.; Watson, D.; Kemner, K. M.; Marsh, T.; Tiedje, J.; Zhou, J. Z.; Fendorf, S.; Kitanidis, P. K.; Jardine, P. M.; Criddle, C. S., In situ bioreduction of uranium (VI) to submicromolar levels and reoxidation by dissolved oxygen. *Environmental Science & Technology* **2007,** *41*, 5716-5723.

[9]   Watson, D. B.; Quarles, H. D. *Environmental Remediation Sciences Program (ERSP) Integrated Field Challenge (IFC) Project and Oak Ridge Field Research Center (ORFRC) Management Plan*; ORNL/TM-2000/267; Oak Ridge National Laboratory: Oak Ridge, TN, 2007.

[10]   Roh, Y.; Lee, S. R.; Choi, S. K.; Elless, M. P.; Lee, S. Y., Physicochemical and mineralogical characterization of uranium-contaminated soils. *Soil & Sediment Contamination* **2000,** *9*, 463-486.

[11]   Stubbs, J. E.; Elbert, D. C.; Veblen, D. R.; Zhu, C., Electron microbeam investigation of uranium-contaminated soils from Oak Ridge, TN, USA. *Environmental Science & Technology* **2006,** *40*, 2108-2113.

[12]   Buck, E. C.; Brown, N. R.; Dietz, N. L., Contaminant uranium phases and leaching at the Fernald site in Ohio. *Environmental Science & Technology* **1996,** *30*, 81-88.

[13]   Buck, E. C.; Dietz, N. L.; Bates, J. K., Uranium-contaminated soils: Ultramicrotomy and electron-beam analysis. *Microscopy Research and Technique* **1995,** *31*, 174-181.

[14]   Morris, D. E.; Allen, P. G.; Berg, J. M.; Chisholm-Brause, C. J.; Conradson, S. D.; Donohoe, R. J.; Hess, N. J.; Musgrave, J. A.; Tait, C. D., Speciation of uranium in Fernald soils by molecular spectroscopic methods: Characterization of untreated soils. *Environmental Science & Technology* **1996,** *30*, 2322-2331.

[15]   Wellman, D. M.; Gunderson, K. M.; Icenhower, J. P.; Forrester, S. W.; Forrester, S. W., Dissolution kinetics of synthetic and natural meta-autunite minerals, $X_{3-n}^{(n)+} [(UO_2)(PO_4)]_2 \cdot xH_2O$, under acidic conditions. *Geochemistry Geophysics Geosystems* **2007,** *8*.

[16]   Wellman, D. M.; Icenhower, J. P.; Gamerdinger, A. P.; Forrester, S. W., Effects of pH, temperature, and aqueous organic material on the dissolution kinetics of meta-autunite minerals, $(Na, Ca)_{2-1}[(UO_2)(PO_4)]_2 \cdot 3H_2O$. *American Mineralogist* **2006,** *91*, 143-158.

[17]   Kelly, S. D.; Kemner, K. M.; Carley, J.; Criddle, C. S.; Jardine, P. M.; Marsh, T. L.; Phillips, D.; Watson, D.; Wu, W. M., Speciation of uranium in sediments before and after in situ biostimulation. *Environmental Science & Technology* **2008,** *42*, 1558-1564.

[18]   Beazley, M. J.; Martinez, R. J.; Sobecky, P. A.; Webb, S. M.; Taillefert, M., Uranium biomineralization as a result of bacterial phosphatase activity: Insights from bacterial isolates from a contaminated subsurface. *Environmental Science & Technology* **2007,** *41*, 5701-5707.

[19]   Zachara, J. M.; Serne, J.; Freshley, M.; Mann, F.; Anderson, F.; Wood, M.; Jones, T.; Myers, D., Geochemical processes controlling migration of tank wastes in Hanford's vadose zone. *Vadose Zone Journal* **2007,** *6*, 985-1003.

[20]   Wellman, D. M.; Icenhower, J. P.; Owen, A. T., Comparative analysis of soluble phosphate amendments for the remediation of heavy metal contaminants: Effect on sediment hydraulic conductivity. *Environmental Chemistry* **2006,** *3*, 219-224.

[21]   Wellman, D. M.; Icenhower, J. P.; Pierce, E. M.; McNamara, B. K.; Burton, S. D.; Geiszler, K. N.; Baum, S. R.; Butler, B. C., Polyphosphate amendments for in-situ immobilization of uranium plumes. In *Third International Conference on Remediation of Contaminated Sediments*, Olfenbuttel, R. F.; White, P. J., Eds. Battelle Press: Columbus, OH, 2005; Vol. 3.

[22]   Wellman, D. M.; Fruchter, J. S.; Vermeul, V. R. *Experimental Plan: Uranium Stabilization Through Polyphosphate Injection 300 Area Uranium Plume Treatability Demonstration Project*; PNNL-16101; Pacific Northwest National Laboratory: Richland, WA, 2006.

[23]   Wellman, D. M.; Glovack, J. N.; Parker, K.; Richards, E. L.; Pierce, E. M., Sequestration and retention of uranium(VI) in the presence of hydroxylapatite under dynamic geochemical conditions. *Environmental Chemistry* **2008,** *5*, 40-50.

[24]   Wellman, D. M.; Pierce, E. M.; Valenta, M. M., Efficacy of soluble sodium tripolyphosphate amendments for the in-situ immobilisation of uranium. *Environmental Chemistry* **2007,** *4*, 293-300.

[25]   Fuller, C. C.; Bargar, J. R.; Davis, J. A.; Piana, M. J., Mechanisms of uranium interactions with hydroxyapatite: Implications for groundwater remediation. *Environmental Science & Technology* **2002,** *36*, 158-165.

[26]   Vermeul, V. R.; Fruchter, J. S.; Wellman, D. M.; Williams, B. A.; Williams, M. D. *Site Characterization Plan: Uranium Stabilization through Polyphosphate Injection - 300*

Area Uranium Plume Treatability Demonstration Project; PNNL-16008; Pacific Northwest National Laboratory: Richland, WA, 2006.

[27] Wellman, D. M.; Pierce, E. M.; Richards, E. L.; Butler, B. C.; Parker, K. E.; Glovack, J. N.; Burton, S. D.; Baum, S. R.; Clayton, E. T.; Rodriguez, E. A. *Interim Report: Uranium Stabilization through Polyphosphate Injection - 300 Area Uranium Plume Treatability Demonstration Project*; PNNL-16683; Pacific Northwest National Laboratory: Richland, WA, 2007.

[28] Gamerdinger, A. P.; Kaplan, D. I.; Wellman, D. M.; Serne, R. J., Two-region flow and rate-limited sorption of uranium (VI) during transport in an unsaturated silt loam. *Water Resources Research* **2001,** *37*, 3147-3153.

[29] Gamerdinger, A. P.; Kaplan, D. I.; Wellman, D. M.; Serne, R. J., Two-region flow and decreased sorption of uranium (VI) during transport in Hanford groundwater and unsaturated sands. *Water Resources Research* **2001,** *37*, 3155-3162.

[30] Grenthe, I.; Fuger, J.; Konings, R. J. M.; Lemire, R. J.; Mueller, A. B.; Nguyen-Trung, C.; Wanner, H., *Chemical Thermodynamics of Uranium*. Elsevier: Amsterdam, 1992.

[31] Guillaumont, R.; Fanghänel, T.; Fuger, J.; Grenthe, I.; Neck, V.; Palmer, D. A.; Rand, M. H.; Mompean, F. J.; Illemassene, M.; Domenech-Orti, C.; Ben-Said, K., *Update on the Chemical Thermodynamics of Uranium, Neptunium, Plutonium, Americium & Technetium*. Elsevier: Amsterdam, 2003.

[32] Felmy, A. R.; Xia, Y. X.; Wang, Z. M., The solubility product of $NaUO_2PO_4 \cdot xH_2O$ determined in phosphate and carbonate solutions. *Radiochimica Acta* **2005,** *93*, 401-408.

[33] Rai, D.; Xia, Y. X.; Rao, L. F.; Hess, N. J.; Felmy, A. R.; Moore, D. A.; McCready, D. E., Solubility of $(UO_2)_3(PO_4)_2 \cdot 4H_2O$ in $H^+-Na^+-OH^--H_2PO_4^--HPO_4^{2-}-PO_4^{3-}-H_2O$ and its comparison to the analogous PuO_2^{2+} system. *Journal of Solution Chemistry* **2005,** *34*, 469-498.

[34] Bernhard, G.; Geipel, G.; Brendler, V.; Nitsche, H., Speciation of uranium in seepage waters of a mine tailing pile studied by time-resolved laser-induced fluorescence spectroscopy (TRLFS). *Radiochimica Acta* **1996,** *74*, 87-91.

[35] Bernhard, G.; Geipel, G.; Reich, T.; Brendler, V.; Amayri, S.; Nitsche, H., Uranyl(VI) carbonate complex formation: Validation of the $Ca_2UO_2(CO_3)_3$(aq.) species. *Radiochimica Acta* **2001,** *89*, 511-518.

[36] Kalmykov, S. N.; Choppin, G. R., Mixed $Ca^{2+}/UO_2^{2+}/CO_3^{2-}$ complex formation at different ionic strengths. *Radiochimica Acta* **2000,** *88*, 603-606.

[37] Dong, W. M.; Brooks, S. C., Determination of the formation constants of ternary complexes of uranyl and carbonate with alkaline earth metals (Mg^{2+}, Ca^{2+}, Sr^{2+}, and Ba^{2+}) using anion exchange method. *Environmental Science & Technology* **2006,** *40*, 4689-4695.

[38] Sandino, A.; Bruno, J., The solubility of $(UO_2)_3(PO_4)_2 \cdot 4H_2O_{(s)}$ and the formation of U(VI) phosphate complexes: Their influence in uranium speciation in natural waters. *Geochimica et Cosmochimica Acta* **1992,** *56*, 4135-4145.

[39] Weigel, F.; Hoffmann, G., Phosphates and arsenates of hexavalent actinides. Part 1. Uranium. *Journal of the Less-Common Metals* **1976,** *44*, 99-123.

[40] Pham-Thi, M.; Colomban, P., Morphological, X-ray and vibrational study of various uranyl phosphate hydrates. *Journal of the Less-Common Metals* **1985,** *108*, 189-216.

[41] Finch, R. J.; Ewing, R. C., The corrosion of uraninite under oxidizing conditions. *Journal of Nuclear Materials* **1992,** *190*, 133-156.

[42]   Benavente, J.; Barrado, J. R. R.; Cabeza, A.; Bruque, S.; Martinez, M., A comparative-study of the electrical behavior of different uranyl phosphate-based membranes by AC and DC measurements. *Colloids and Surfaces, A: Physicochemical and Engineering Aspects* **1995,** *97*, 13-20.

[43]   Dieckmann, G. H.; Ellis, A. B., Interlamellar Liebig Titration Based on Photoluminescence - Reaction of Silver Uranyl Phosphate with Hydrogen-Cyanide Gas. *Inorganic Chemistry* **1987,** *26*, 4147-4148.

[44]   Fairchild, J. G., Base exchange in artificial autunites. *American Mineralogist* **1929,** *14*, 265-275.

[45]   Hunsberger, L. R.; Ellis, A. B., Excited-State Properties of Lamellar Solids Derived from Metal-Complexes and Hydrogen Uranyl Phosphate. *Coordination Chemistry Reviews* **1990,** *97*, 209-224.

[46]   Vochten, R., Transformation of chernikovite and sodium autunite into lehnerite. *American Mineralogist* **1990,** *75*, 221-225.

[47]   Locock, A. J.; Burns, P. C., The crystal structure of synthetic autunite, $Ca[(UO_2)(PO_4)]_2(H_2O)_{11}$. *American Mineralogist* **2003,** *88*, 240-244.

[48]   Locock, A. J.; Burns, P. C., Crystal structures and synthesis of the copper-dominant members of the autunite and meta-autunite groups: Torbernite, zeunerite, metatorbernite and metazeunerite. *Canadian Mineralogist* **2003,** *41*, 489-502.

[49]   Locock, A. J.; Burns, P. C.; Duke, M. J. M.; Flynn, T. M., Monovalent cations in structures of the meta-autunite group. *Canadian Mineralogist* **2004,** *42*, 973-996.

[50]   Locock, A. J.; Burns, P. C.; Flynn, T. M., Divalent transition metals and magnesium in structures that contain the autunite-type sheet. *Canadian Mineralogist* **2004,** *42*, 1699-1718.

[51]   Locock, A. J.; Burns, P. C.; Flynn, T. M., Structures of strontium- and barium-dominant compounds that contain the autunite-type sheet. *Canadian Mineralogist* **2005,** *43*, 721-733.

[52]   Locock, A. J.; Burns, P. C., The crystal structure of triuranyl diphosphate tetrahydrate. *Journal of Solid State Chemistry* **2002,** *163*, 275-280.

[53]   Davis, J. A. *Surface complexation modeling of uranium (VI) adsorption on natural mineral assemblages*; NUREG/CR-6708; Division of Risk Analysis and Applications, Office of Nuclear Regulatory Research, U.S. Nuclear Regulatory Commission: Washington, DC, March 2001, 2001; p 214.

[54]   Cheng, T.; Barnett, M. O.; Roden, E. E.; Zhuang, J. L., Effects of phosphate on uranium(VI) adsorption to goethite-coated sand. *Environmental Science & Technology* **2004,** *38*, 6059-6065.

[55]   Payne, T. E.; Davis, J. A.; Waite, T. D., Uranium adsorption on ferrihydrite: Effects of phosphate and humic acid. *Radiochimica Acta* **1996,** *74*, 239-243.

[56]   Guo, Z. L.; Guo, F. H.; Tao, Z. Y., Effects of phosphate and ionic strength upon uranium(VI) sorption onto alumina as a function of pH. *Radiochimica Acta* **2006,** *94*, 223-228.

[57]   Romero-Gonzalez, M. R.; Cheng, T.; Barnett, M. O.; Roden, E. E., Surface complexation modeling of the effects of phosphate on uranium(VI) adsorption. *Radiochimica Acta* **2007,** *95*, 251-259.

[58]   Cheng, T.; Barnett, M. O.; Roden, E. E.; Zhunag, J. L., Reactive transport of uranium(VI) and phosphate in a goethite-coated sand column: An experimental study. *Chemosphere* **2007,** *68*, 1218-1223.

[59]   Singh, A.; Giammar, D. E., Adsorption and surface precipitation of uranyl phosphate on goethite. In *233rd American Chemical Society National Meeting*, Chicago, Illinois, 2007; Vol. ENVR-211.

[60]   Fuller, C. C.; Bargar, J. R.; Davis, J. A., Molecular-scale characterization of uranium sorption by bone apatite materials for a permeable reactive barrier demonstration. *Environmental Science & Technology* **2003,** *37*, 4642-4649.

[61]   Murakami, T.; Sato, T.; Ohnuki, T.; Isobe, H., Field evidence for uranium nanocrystallization and its implications for uranium transport. *Chemical Geology* **2005,** *221*, 117-126.

[62]   Sowder, A. G.; Clark, S. B.; Fjeld, R. A., The impact of mineralogy in the U(VI)-Ca-PO_4 system on the environmental availability of uranium. *Journal of Radioanalytical and Nuclear Chemistry* **2001,** *248*, 517-524.

[63]   Sowder, A. G.; Clark, S. B.; Field, R. A., The transformation of uranyl oxide hydrates: The effect of dehydration on synthetic metaschoepite and its alteration to becquerelite. *Environmental Science & Technology* **1999,** *33*, 3552-3557.

[64]   Finch, R. J.; Miller, M. L.; Ewing, R. C., Weathering of natural uranyl oxide hydrates: Schoepite polytypes and dehydration effects. *Radiochimica Acta* **1992,** *58-9*, 433-443.

[65]   Schindler, M.; Hawthorne, F. C.; Burns, P. C.; Maurice, P. A., Dissolution of uranyl-oxide-hydroxy-hydrate minerals. II. Becquerelite. *Canadian Mineralogist* **2006,** *44*, 1207-1225.

[66]   Schindler, M.; Hawthorne, F. C.; Burns, P. C.; Maurice, P. A., Dissolution of uranyl-oxide-hydroxy-hydrate minerals. IV. Fourmarierite and synthetic $Pb_2(H_2O)[(UO_2)_{10}UO_{12}(OH)_6(H_2O)_2]$. *Canadian Mineralogist* **2007,** *45*, 963-981.

[67]   Schindler, M.; Hawthorne, F. C.; Halden, N. M.; Burns, P. C.; Maurice, P. A., Dissolution of uranyl-oxide-hydroxy-hydrate minerals. III. Billietite. *Canadian Mineralogist* **2007,** *45*, 945-962.

[68]   Schindler, M.; Mandaliev, P.; Hawthorne, F. C.; Putnis, A., Dissolution of uranyl-oxide-hydroxy-hydrate minerals. I. Curite. *Canadian Mineralogist* **2006,** *44*, 415-431.

[69]   Steefel, C. I.; Vancappellen, P., A new kinetic approach to modeling water-rock interaction: The role of nucleation, precursors, and Ostwald pipening. *Geochimica et Cosmochimica Acta* **1990,** *54*, 2657-2677.

[70]   Lower, S. K.; Maurice, P. A.; Traina, S. J.; Carlson, E. H., Aqueous Pb sorption by hydroxylapatite: Application of atomic force microscopy to dissolution, nucleation, and growth studies. *American Mineralogist* **1998,** *83*, 147-158.

[71]   Manecki, M.; Maurice, P. A.; Traina, S. J., Uptake of aqueous Pb by Cl^-, F^-, and OH^- apatites: Mineralogic evidence for nucleation mechanisms. *American Mineralogist* **2000,** *85*, 932-942.

[72]   Fenter, P.; Cheng, L.; Park, C.; Zhang, Z.; Sturchio, N. C., Structure of the orthoclase (001)- and (010)-water interfaces by high-resolution X-ray reflectivity. *Geochimica Et Cosmochimica Acta* **2003,** *67*, 4267-4275.

[73]   Fenter, P.; Teng, H.; Geissbuhler, P.; Hanchar, J. M.; Nagy, K. L.; Sturchio, N. C., Atomic-scale structure of the orthoclase (001)-water interface measured with high-resolution X-ray reflectivity. *Geochimica et Cosmochimica Acta* **2000,** *64*, 3663-3673.

[74] Serne, R. J.; Brown, C. F.; Schaef, H. T.; Pierce, E. P.; Lindberg, M. J.; Wang, Z.; Gassman, P.; Catalano, J. G. *300 Area Uranium Leach and Adsorption Project: ERC FY01-02 Final Report*; PNNL-14022; United States Department of Energy, Richland Operations: Richland, WA, 2002.

[75] Cheng, L.; Fenter, P.; Nagy, K. L.; Schlegel, M. L.; Sturchio, N. C., Molecular-scale density oscillations in water adjacent to a mica surface. *Physical Review Letters* **2001,** *87,* 156103.

[76] Park, C.; Fenter, P. A.; Nagy, K. L.; Sturchio, N. C., Hydration and distribution of ions at the mica-water interface. *Physical Review Letters* **2006,** *97,* 016101.

[77] Schlegel, M. L.; Nagy, K. L.; Fenter, P.; Cheng, L.; Sturchio, N. C.; Jacobsen, S. D., Cation sorption on the muscovite (001) surface in chloride solutions using high-resolution X-ray reflectivity. *Geochimica Et Cosmochimica Acta* **2006,** *70,* 3549-3565.

[78] Catalano, J. G.; Brown, G. E., Jr., Uranyl adsorption onto montmorillonite: Evaluation of binding sites and carbonate complexation. *Geochimica et Cosmochimica Acta* **2005,** *69,* 2995-3005.

[79] McKinley, J. P.; Zachara, J. M.; Smith, S. C.; Turner, G. D., The influence of uranyl hydrolysis and multiple site-binding reactions on adsorption of U(VI) to montmorillonite. *Clays and Clay Minerals* **1995,** *43,* 586-598.

[80] Pabalan, R. T.; Turner, D. R., Uranium(6+) sorption on montmorillonite: Experimental and surface complexation modeling study. *Aquatic Geochemistry* **1997,** *2,* 203-226.

[81] Turner, G. D.; Zachara, J. M.; McKinley, J. P.; Smith, S. C., Surface-charge properties and UO_2^{2+} adsorption of a subsurface smectite. *Geochimica et Cosmochimica Acta* **1996,** *60,* 3399-3414.

[82] Zachara, J. M.; McKinley, J. P., Influence of hydrolysis on the sorption of metal-cations by smectites: Importance of edge coordination reactions. *Aquatic Sciences* **1993,** *55,* 250-261.

[83] Catalano, J. G.; Fenter, P.; Park, C., Structural comparison of the hematite and alumina (110)-water interfaces. *Geochimica et Cosmochimica Acta* **2008**.

[84] Xie, L.; Giammar, D. E., Influence of phosphate on adsorption and surface precipitation of lead on iron oxide surfaces. In *Adsorption of Metals by Geomedia II*, Barnett, M. O.; Kent, D. B., Eds. Elsevier: Amsterdan, The Netherlands, 2008; Vol. 7, pp 349-373.

[85] Bethke, C. M. *The Geochemists Workbench. A user's guide to Rxn, Act2, Tact, React, and Gtplot*; University of Illinois, 2001.

[86] Schecher, W. D.; McAvoy, D. C. *MINEQL+: A chemical equilibrium modeling system, version 4.5*, 4.5; Environmental Research Software: Hallowell, ME, 1998.

[87] McGrail, B. P.; Martin, P. F. C.; Lindenmeier, C. W., Accelerated Testing of Waste Forms Using a Novel Pressurized Unsaturated Flow (Puf) Method. *Materials Research Society Symposium Proceedings* **1997**.

[88] McGrail, B. P.; Martin, P. F. C.; Lindenmeier, C. W. Method and Apparatus for Measuring Coupled Flow, Transport, and Reaction Processes under Liquid Unsaturated Flow Conditions. Patent No. 5974859, 1999.

[89] Pierce, E. M.; McGrail, B. P.; Valenta, M. M.; Strachan, D. M., The accelerated weathering of a radioactive low-activity waste glass under hydraulically unsaturated conditions: Experimental results from a pressurized unsaturated flow test. *Nuclear Technology* **2006,** *155,* 149-165.

[90] Wierenga, P. J.; Vangenuchten, M. T., Solute Transport through Small and Large Unsaturated Soil Columns. *Ground Water* **1989,** *27*, 35-42.

[91] Pierce, E. M.; McGrail, B. P.; Bagasen, L. M.; Rodriguez, E. A.; Wellman, D. M.; Geizler, K. N.; Baum, S. R.; Reed, L. R.; Crum, J. V.; Schaef, H. T. *Laboratory Testing of Bulk Vitrified Low-Activity Waste Forms to Support the 2005 Integrated Disposal Facility Performance Assessment*; PNNL-15126; Pacific Northwest National Laboratory: Richland, WA, 2005.

[92] Pierce, E. M.; McGrail, B. P.; Martin, P. F.; Marra, J.; Arey, B. W.; Geiszler, K. N., Accelerated weathering of high-level and plutonium-bearing lanthanide borosilicate waste glasses under hydraulically unsaturated conditions. *Applied Geochemistry* **2007,** *22*, 1841-1859.

[93] Sutton, S. R.; Bertsch, P. M.; Newville, M.; Rivers, M.; Lanzirotti, A.; Eng, P. J., Microfluorescence and microtomography analyses of heterogeneous earth and environmental materials. *Reviews in Mineralogy and Geochemistry* **2002,** *49*, 429-483.

[94] Fenter, P.; Park, C.; Cheng, L.; Zhang, Z.; Krekeler, M. P. S.; Sturchio, N. C., Orthoclase dissolution kinetics probed by in situ X-ray reflectivity: Effects of temperature, pH, and crystal orientation. *Geochimica et Cosmochimica Acta* **2003,** *67*, 197-211.

[95] Teng, H. H.; Fenter, P.; Cheng, L. W.; Sturchio, N. C., Resolving orthoclase dissolution processes with atomic force microscopy and X-ray reflectivity. *Geochimica et Cosmochimica Acta* **2001,** *65*, 3459-3474.

[96] Morosin, B., Hydrogen uranyl phosphate tetrahydrate, a hydrogen-ion solid electrolyte. *Acta Crystallographica* **1978,** *34*, 3732-3734.

[97] Giammar, D. E.; Hering, J., Dissolution and transformation rates of uranyl mineral phases. *Abstracts of Papers of the American Chemical Society* **2000,** *220*, 153-ENVR.

[98] Giammar, D. E.; Hering, J. G., Equilibrium and kinetic aspects of soddyite dissolution and secondary phase precipitation in aqueous suspension. *Geochimica et Cosmochimica Acta* **2002,** *66*, 3235-3245.

[99] Lasaga, A. C., Fundamental approaches in describing mineral dissolution and precipitation rates. In *Chemical weathering rates of silicate minerals*, White, A. F.; Brantley, S. L., Eds. Mineralogical Society of America: Washington, D.C., 1995; Vol. 31, pp 23-86.

[100] Lasaga, A. C., *Kinetic theory in the earth sciences*. Princeton University Press: Princeton, New Jersey, 1998; p 811.

[101] Ilton, E. S.; Qafoku, N. P.; Liu, C.; Moore, D. A.; Zachara, J. M., Advective removal of intraparticle uranium from contaminated vadose zone sediments, Hanford, U.S. *Environmental Science & Technology* **2008,** *42*, 1565-1571.

[102] Liu, C. X.; Zachara, J. M.; Qafoku, O.; McKinley, J. P.; Heald, S. M.; Wang, Z. M., Dissolution of uranyl microprecipitates in subsurface sediments at Hanford site, USA. *Geochimica et Cosmochimica Acta* **2004,** *68*, 4519-4537.

[103] Catalano, J. G.; Brown, G. E., Jr., Analysis of uranyl-bearing phases by EXAFS spectroscopy: Interferences, multiple scattering, accuracy of structural parameters, and spectral differences. *American Mineralogist* **2004,** *89*, 1004-1021.

[104] Waychunas, G. A., Grazing-incidence X-ray absorption and emission spectroscopy. *Reviews in Mineralogy and Geochemistry* **2002,** *49*, 267-315.

[105] Fenter, P., X-ray reflectivity as a probe of mineral-fluid interfaces: A user guide. *Reviews in Mineralogy and Geochemistry* **2002,** *49*, 149-220.

[106]   Catalano, J. G.; Heald, S. M.; Zachara, J. M.; Brown, G. E., Spectroscopic and diffraction study of uranium speciation in contaminated vadose zone sediments from the Hanford site, Washington state. *Environmental Science & Technology* **2004,** *38*, 2822-2828.

[107]   McKinley, J. P.; Zachara, J. M.; Liu, C. X.; Heald, S. C.; Prenitzer, B. I.; Kempshall, B. W., Microscale controls on the fate of contaminant uranium in the vadose zone, Hanford Site, Washington. *Geochimica et Cosmochimica Acta* **2006,** *70*, 1873-1887.

[108]   Schindler, M.; Hawthorne, F. C.; Putnis, C.; Putnis, A., Growth of uranyl-hydroxy-hydrate and uranyl-carbonate minerals on the (104) surface of calcite. *Canadian Mineralogist* **2004,** *42*, 1683-1697.

[109]   Zachara, J. M.; Ainsworth, C. C.; Brown, G. E., Jr.; Catalano, J. G.; McKinley, J. P.; Qafoku, O.; Smith, S. C.; Szecsody, J. E.; Traina, S. J.; Warner, J. A., Chromium speciation and mobility in a high level nuclear waste vadose zone plume. *Geochimica et Cosmochimica Acta* **2004,** *68*, 13-30.

[110]   Catalano, J. G.; Park, C.; Fenter, P.; Zhang, Z., Simultaneous inner- and outer-sphere arsenate complexation on corundum and hematite. *Geochimica et Cosmochimica Acta* **2008**, doi: 10.1016/j.gca.2008.02.013.

[111]   Catalano, J. G.; Trainor, T. P.; Eng, P. J.; Waychunas, G. A.; Brown, G. E., Jr., CTR diffraction and grazing-incidence EXAFS study of U(VI) adsorption onto α-Al$_2$O$_3$ and α-Fe$_2$O$_3$ (1-102) surfaces. *Geochimica et Cosmochimica Acta* **2005,** *69*, 3555-3572.

[112]   Catalano, J. G.; Zhang, Z.; Fenter, P.; Bedzyk, M. J., Inner-sphere adsorption geometry of Se(IV) at the hematite (100)-water interface. *Journal of Colloid and Interface Science* **2006,** *297*, 665-671.

[113]   Catalano, J. G.; Zhang, Z.; Park, C.; Fenter, P.; Bedzyk, M. J., Bridging arsenate surface complexes on the hematite (012) surface. *Geochimica et Cosmochimica Acta* **2007,** *71*, 1883-1897.

[114]   Zhang, Z.; Fenter, P.; Kelly, S. D.; Catalano, J. G.; Bandura, A. V.; Kubicki, J. D.; Sofo, J. O.; Wesolowski, D. J.; Machesky, M. L.; Sturchio, N. C.; Bedzyk, M. J., Structure of hydrated Zn^{2+} at the rutile TiO$_2$ (110)-aqueous solution interface: Comparison of X-ray standing wave, X-ray absorption spectroscopy, and density functional theory results. *Geochimica et Cosmochimica Acta* **2006,** *70*, 4039-4056.

[115]   Catalano, J. G.; Warner, J. A.; Brown, G. E., Jr., Sorption and precipitation of Co(II) in Hanford sediments and alkaline aluminate solutions. *Applied Geochemistry* **2005,** *20*, 193-205.

[116]   Catalano, J. G.; Fenter, P.; Park, C., Interfacial water structure on the (012) surface of hematite: Ordering and reactivity in comparison with corundum. *Geochimica et Cosmochimica Acta* **2007,** *71*, 5313-5324.

[117]   Catalano, J. G.; Park, C.; Zhang, Z.; Fenter, P., Termination and water adsorption at the α-Al$_2$O$_3$ (012) - aqueous solution interface. *Langmuir* **2006,** *22*, 4668-4673.

[118]   Zeng, H.; Fisher, B.; Giammar, D. E., Individual and competitive adsorption of arsenate and phosphate to a high-surface-area iron oxide-based sorbent. *Environmental Science & Technology* **2008,** *42*, 147-152.

[119]   Xie, L.; Giammar, D. E., Equilibrium solubility and dissolution rate of the lead phosphate chloropyromorphite. *Environmental Science & Technology* **2007,** *41*, 8050-8055.

[120]   Giammar, D. E.; Hering, J. G., Influence of dissolved sodium and cesium on uranyl oxide hydrate solubility. *Environmental Science & Technology* **2004,** *38*, 171-179.

[121] Giammar, D. E.; Xie, L.; Pasteris, J. D., Immobilization of lead with nanocrystalline carbonated apatite present in fish bone. *Environmental Engineering Science* **2008**, in press.

[122] Wellman, D. M.; Catalano, J. G.; Icenhower, J. P.; Gamerdinger, A. P., Synthesis and characterization of sodium meta-autunite, $NaUO_2PO_4 \cdot 3H_2O$. *Radiochimica Acta* **2005,** *93*, 393-399.

[123] Wellman, D. M.; Icenhower, J. P.; Weber, W. J., Elemental dissolution study of Pu-bearing borosilicate glasses. *Journal of Nuclear Materials* **2005,** *340*, 149-162.

[124] Wellman, D. M.; Pierce, E. M.; Oostrom, M.; Fruchter, J. S. *Experimental Plan: 300 Area Treatability Test: In Situ Treatment of the Vadose Zone and Smear Zone Uranium Contamination by Polyphosphate Infiltration*; PNNL-16823; Pacific Northwest National Laboratory: Richland, WA, 2007.

APPENDIX B: BIOGRAPHICAL SKETCHES/CONFLICTS OF INTEREST

JEFFREY G. CATALANO

Department of Earth and Planetary Sciences
Washington University in St. Louis
Saint Louis MO 63130-4862
Tel.: (314) 935-6015
Fax.: (314) 935-7361
E-mail: catalano@wustl.edu

Education: B.S. Geology, 1999, University of Illinois at Urbana-Champaign; Ph.D. Geological and Environmental Sciences, 2004, Stanford University; Postdoctoral Fellow, Argonne National Laboratory, 2004-2007.

Appointments: Assistant Professor, Department of Earth and Planetary Sciences, Washington University in St. Louis (2007-present); Harold Urey Postdoctoral Fellow, Environmental Research and Chemistry Divisions, Argonne National Laboratory (2004-2007); Graduate Teaching Assistant and Graduate Research Assistant, Department of Geological and Environmental Sciences, Stanford University (1999-2004); Student Assistant, US Geological Survey, Water Resources Division, Illinois Water Science Center, Urbana, IL (1997-1999).

Awards and Honors: Harold Urey Postdoctoral Fellowship, Argonne National Laboratory (2004-2007), Corning Foundation Science Fellow, Stanford University (2000-2001)

Ten Relevant Publications:
Dr. Catalano has published 24 journal articles and 4 technical reports

Catalano J.G., Park C., Fenter P., Zhang Z. (2008) Simultaneous inner- and outer-sphere arsenate adsorption on corundum and hematite. *Geochimica et Cosmochimica Acta*, doi: 10.1016/j.gca.2008.02.013.

Catalano J.G., Park C., Fenter P. (2007) Interfacial water structure on the (012) surface of hematite: Ordering and reactivity in comparison with corundum. *Geochimica et Cosmochimica Acta* **71**, 5313-5324.

Catalano J.G., McKinley J.P., Zachara J.M., Heald S.M., Smith S.C., and Brown G.E., Jr. (2006) Changes in uranium speciation through a depth sequence of contaminated Hanford sediments. *Environmental Science & Technology* **40**, 2517-2524.

Wellman D.M., **Catalano J.G.**, Icenhower J.P., and Gamerdinger A.P. (2005) Synthesis and characterization of sodium meta-autunite, $Na_2[(UO_2)(PO_4)]_2 \cdot 3H_2O$. *Radiochimica Acta* **93**, 393-399.

Catalano J.G., Trainor T.P., Eng P.J., Waychunas G.A., and Brown G.E., Jr. (2005) CTR diffraction and grazing-incidence EXAFS study of U(VI) adsorption onto α-Al_2O_3 and α-Fe_2O_3 ($1\bar{1}02$) surfaces. *Geochimica et Cosmochimica Acta* **69**, 3555-3572.

Catalano J.G., and Brown G.E., Jr. (2005) Uranyl adsorption onto montmorillonite: Evaluation of binding sites and carbonate complexation. *Geochimica et Cosmochimica Acta* **69**, 2995-3005.

Catalano J.G., Warner J.A., and Brown G.E., Jr. (2005) Sorption and precipitation of Co(II) in Hanford sediments and alkaline aluminate solutions. *Applied Geochemistry* **20**, 193-205.

Catalano J.G., and Brown G.E., Jr. (2004) Analysis of uranyl-bearing phases by EXAFS spectroscopy: Interferences, multiple scattering, accuracy of structural parameters, and spectral differences. *American Mineralogist* **89**, 1004-1021.

Catalano J.G., Heald S.M., Zachara J.M., and Brown G.E., Jr. (2004) Spectroscopic and diffraction study of uranium speciation in contaminated vadose zone sediments from the Hanford Site, Washington State. *Environmental Science & Technology* **38**, 2822-2828.

Zachara J.M., Ainsworth C.C., Brown G.E., Jr., **Catalano J.G.**, McKinley J.P., Qafoku O., Smith S.C., Szecsody J.E., Traina S.J., and Warner J.A. (2004) Chromium speciation and mobility in a high level nuclear waste vadose zone plume. *Geochimica et Cosmochimica Acta* **68**, 13-30.

Synergistic Activities: Reviewer, U.S. Civilian Research and Development Foundation; Reviewer, Stanford Synchrotron Radiation Laboratory user proposals; Reviewer for Scholarly Journals (*American Mineralogist, Chemical Geology, Environ. Sci. Technol., Geochemical Journal, Geochim. Cosmochim. Acta, Geology, Journal of Colloid and Interface Science, Journal of Environmental Management, Journal of Environmental Radioactivity, Journal of Hazardous Materials, Science of the Total Environment, Thermochimica Acta*).

Collaborators in the Last 36 Months:
Bandura, A. (St. Petersburg State U.), Bedzyk, M.J. (Northwestern U.), Benzerara, K. (U. Paris 6-7), Bluhm, H. (LBNL), Brown, G.E., Jr. (Stanford U.), Calas, G. (U. Paris 6-7), Cances, B. (U. Reims), Chaka, A.M. (NIST), Eng, P.J. (U. Chicago), Farges, F. (Mus. Nat. d'Histoire Naturelle), Fenter, P. (ANL), Giammar, D.E. (Washington Univ.), Ghose, S.K. (U. Chicago), Heald, S.M. (ANL), Juillot, F. (U. Paris 6-7), Jun, Y.-S. (Washington Univ.), Kelly, S.D. (ANL), Kendelewicz, T. (Stanford U.), Kubicki, J.D. (Penn State U.), Lo, C. (Washington U.), Machesky, M.L. (ISWS), McKinley, J.P. (PNNL), Morin, G. (U. Paris 6-7), Nagy, K.L. (U. Illinois), Nilsson, A. (SSRL), Ona-Nguema, G. (Stanford U.), Park, C. (ANL), Pasteris, J.D. (Washington Univ.), Petitto, S.C. (U. Alaska), Pierce, E.M. (PNNL), Salmeron, M. (LBNL), Smith, S.C. (PNNL), Sofo, J. (Penn State U.), Starr, D.E. (LBNL), Sturchio, N.C. (U. Illinois), Tanwar, K. (U. Alaska), Trainor, T.P. (U. Alaska), Valenta, M.M. (PNNL), Waychunas, G.A. (LBNL), Wellman, D.M. (PNNL), Wesolowski, D.J. (ORNL), Yamamoto, S. (SSRL), Yoon, T.Y. (Hanyang U.), Zachara, J.M. (PNNL), Zhang, Z. (ANL)

Ph.D. Advisor: Dr. Gordon E. Brown, Jr., Stanford University

Postdoctoral Advisor: Dr. Paul Fenter, Argonne National Laboratory

Former and Current Graduate and Postdoctoral Students: None

APPENDIX C: FACILITIES, RESOURCES, AND MAJOR EQUIPMENT

Research will be performed at Washington University, Argonne National Laboratory, and Pacific Northwest National Laboratory, with additional measurements made at DOE-supported national user facilities such as the Advanced Photon Source. Research facilities and other resources available are summarized below.

WASHINGTON UNIVERSITY

Environmental Geochemistry and Mineralogy Laboratory
Dr. Catalano's Environmental Geochemistry and Mineralogy Laboratory is located in the new Earth and Planetary Sciences building and includes a general purpose wet chemical laboratory, equipped with standard equipment needed for solution chemistry, mineral-water interface geochemistry, and sample preparation. This equipment includes an two fume hoods, an anaerobic chamber, pH meters, analytical balances, UV/Vis spectrophotometer, wheel and fixture for polishing crystalline substrates, muffle and tube furnaces, ultrapure water system, centrifuges, syringe pumps, etc. The laboratory just received a new Agilent Technologies (formerly Molecular Imaging) atomic force microscope (AFM) model 5500, capable of imaging mineral surfaces under aqueous conditions. The laboratory also maintains computing facilities needed for analysis of X-ray scattering and spectroscopic data and geochemical modeling, as well as equipment needed for making XANES, EXAFS, XR, and RAXR measurements at X-ray light sources.

Aquatic Chemistry Laboratory
Dr. Giammar's Aquatic Chemistry Laboratory is a recently renovated 650 sq. ft. space with state of the art facilities. The laboratory is equipped with two fume hoods, purified air, vacuum, deionized water, and a point-of-use ultrapure (18.2 $M\Omega$-cm) water system. The laboratory has an environmental chamber for conducting experiments at anaerobic or carbon dioxide-free conditions. The laboratory contains all of the equipment necessary for conducting a large set of bench-scale and column experiments including pH meters, magnetic stir plates, peristaltic pumps, fraction collectors, a general purpose centrifuge, an orbital shaker, temperature control baths, and a drying oven. The laboratory also houses a freeze-drier for the preparation and isolation of fine particles in aqueous suspension.

Department of Earth and Planetary Sciences
The department of Earth and Planetary Sciences maintains microscopic, spectroscopic, and diffraction facilities for sample characterization. A new JEOL-8200 electron microprobe is available for element mapping and quantitative compositional analysis of solids. X-ray powder diffraction is done on a Rigaku Geigerflex D-MAX/A Diffractometer using Cu-Ka radiation. The instrument is equipped with a vertical goniometer and a scintillation counter. Maximum power is 1.5kW operating at 50kV and 50mA. PC-based Datascan software by Materials Data, Inc. (MDI) controls the diffractometer and MDI's Jade software can be used to analyze mineral diffraction patterns. A Nicolet Nexus 670 FTIR spectrometer with ATR accessory and a HoloLab 5000 Raman microprobe are available for vibrational spectroscopy measurements.

Department of Energy, Environmental, and Chemical Engineering

Shared analytical facilities in the Department of Energy, Environmental, and Chemical Engineering include the Environmental Nanoscale Analysis Laboratory and the Jens Environmental Engineering Laboratory. These laboratories are common, centralized facilities maintained by full time technicians. Analytical equipment housed in these laboratories include a BET surface area analyzer, an inductively coupled plasma mass spectrometer (ICP-MS), a 96-well plate reader, an atomic absorbance spectrophotometer, a UV-visible spectrophotometer, three gas chromatographs (equipped with flame-ionization, photo-ionization, electron-capture, and thermal-conductivity detectors), a high-performance liquid chromatograph (HPLC) with diode array detector, and a Fourier transform infrared spectrometer with accessories for the analysis of solids, liquids, and suspensions. The department also maintains a Hitachi model S-4500 Field Emission Scanning Electron Microscope with a NORAN Instruments Energy Dispersive X-ray (EDX) microanalysis system.

Center for Material Innovation (CMI)

A JEOL 2100F transmission electron microscope is available through the Center for Materials Innovation, an interdisciplinary research effort of which Drs. Catalano and Giammar are members. The TEM is equipped with an energy-dispersive X-ray spectrometer for analysis of composition in few-nm sized volumes, an electron-energy-loss spectrometer, a high resolution CCD camera, and a film camera for recording diffraction patterns.

Laboratory for Space Sciences

A Cameca IMS 3f SIMS ion microprobe, a Cameca NanoSIMS 50 ion microprobe with high mass resolution multicollector, and a PHI 700 Scanning Auger Nanoprobe are available for use through collaborative agreement with the Laboratory for Space Sciences.

PACIFIC NORTHWEST NATIONAL LABORATORY

Reaction Kinetics Laboratory

Equipment and instrumentation is maintained in a dedicated solid/liquid reaction kinetics laboratory at PNNL for conducting this study of dissolution kinetics of glasses and minerals, including unique equipment for conducting both static and dynamic tests. Our single-pass flow-through (SPFT) system has a capacity of 350 individual cells so that 74 different solutions can be run simultaneously at a given temperature. Fluid delivery systems include 50 precision multiport Kloehn syringe pumps and 24 microinfusion pumps, all delivering steady-state flow rate to within ±1%.

The Pressurized Unsaturated Flow (PUF) test is a novel technique developed at PNNL for testing waste forms (McGrail et al. 1997a; Pierce et al. 2007; Pierce et al. 2006). Our laboratory maintains 16 independent PUF systems. The experimental design provides a unique way to study waste form corrosion behavior and open-system flow and transport hydraulically unsaturated conditions. Like the SPFT test, the PUF test provides multiple degrees of freedom for parameter variation (e.g. chemical affinity, temperature, surface area, and flow rate).

The basic test apparatus consists of a column packed with glass particles (or other material) of a known size and density, and a computer data acquisition and control system. The column is fabricated from a chemically inert material so that dissolution reactions are not

influenced by interaction with the column. A porous titanium plate of proprietary design is sealed in the bottom of the column to ensure an adequate pressure differential for the conductance of fluid while operating under unsaturated conditions. Titanium was chosen because it is highly corrosion resistant and has excellent wetting properties. When water saturated, the porous plate allows water but not air to flow through it, as long as the applied pressure differential does not exceed the air entry relief pressure or "bubble pressure" of the plate. The computer control system runs LabVIEW™ (National Instruments Corporation) software for logging test data to disk from several thermocouples, pressure sensors, inline sensors for effluent pH and conductivity, and column weight from an electronic balance to accurately track water mass balance and saturation level.

Solubility Measurement Laboratory

We maintain state-of-the-art equipment to conduct mineral and compound solubility studies including specially designed Parr reactors. These reactors are equipped to conduct solubility studies at temperatures ranging from $0º – 400º$ C. For conducting kinetic studies above boiling temperatures, a set of reactors are equipped with specialized devices that can collect filtered sample solutions *in-situ* without interrupting the reaction progress. To conduct mineral solubility studies while controlling the water activity in the equilibrating solution, our laboratory is equipped with an isopiestic apparatus consisting of an evacuable stainless steel chamber with twelve vitreous carbon sample cups recessed into an aluminum heating block with a temperature range from ambient to $95º$ C. The activity of water in the reaction chamber can be controlled by isopiestic standard solutions that include KCl, $NaCl$, $CaCl_2$, or H_2SO_4.

Environmental Sciences Laboratory

The Environmental Sciences Laboratory facilities include laboratories for conducting radiological ("hot") and non-radiological ("cold") studies. These facilities are equipped with double-HEPA filtered hoods and controlled atmospheric chambers to permit safe handling of hazardous dispersible materials and completion of characterization and retardation studies under inert or anoxic atmospheric conditions, respectively. The facilities are fully equipped with following instrumentation.

a)   Laboratory analyses of trace metals, hazardous organic and inorganic species, major cations and anions in water and other solution samples
- Inductively coupled plasma - mass spectroscopy (ICP-MS)
- Inductively coupled plasma - optical emission spectroscopy (ICP-OES)
- Ion chromatography (IC)
- UV-VIS spectroscopy, gas chromatography mass spectrometry (GC-MS)
- Fourier transform infrared spectrometry (FTIR)
- High performance liquid chromatography (HPLC)

b) Determining the composition of materials
- X-ray diffraction (XRD)* - crystallography
- X-ray fluorescence (XRF) - Non destructive chemical analysis
- Scanning electron microscopy (SEM) with energy dispersive spectroscopy (EDS)
- Transmission electron microscope (TEM) with energy dispersive spectroscopy (EDS)

      *The XRD capabilities include expertise and established procedures for quantification of the clay mineralogy in soils and sediments, and JADE phase matching software for identification of measured diffraction patterns by comparison to patterns contained in the International Centre for Diffraction Data (ICDD) Powder Diffraction File (PDF).

NATIONAL USER FACILITIES

Advanced Photon Source, Argonne National Laboratory
The APS is a DOE-supported national user facility for the study of matter using brilliant X-ray beams. Users may access this facility at no cost through a competitive, peer-reviewed proposal system. The EXAFS measurements described in this proposal can be performed at a numbers of different beamlines, including 5-BM, 10-ID, 12-BM, 13-BM, 13-ID, 20-BM, and 20-ID; X-ray microprobe measurements at 10-ID, 13-ID, 20-BM, 20-ID; and XR measurements at 5-ID, 6-ID, 11-ID, 12-BM, 13-ID, 20-ID, and 33-ID-D.

APPENDIX D: CURRENT AND PENDING SUPPORT

Investigator: Jeffrey Catalano	Other agencies (including NSF) to which this proposal has

Support: ☐ Current ☒ Pending ☐ Submission Planned in Near Future ☐ *Transfer of Support				
Project/Proposal Title:				
Water Ordering and Complex Oxoanion Absorption Behavior at Iron and Aluminum Oxide-Water Interfaces				
Source of Support: Department of Energy				
Total Award Amount: $420,863 Total Award Period Covered: 9/1/08- 8/31/11				
Location of Project: Washington University				
Person-Months Per Year Committed to the Project. Cal: Acad: Sumr: 1.0				
Support: ☐ Current ☒ Pending ☐ Submission Planned in Near Future ☐ *Transfer of Support				
Project/Proposal Title:				
Iron Oxide Morphology and Composition as Possible Indicators of Sedimentary Redox Cycling				
Source of Support: American Chemical Society				
Total Award Amount: $50,000 Total Award Period Covered: 9/1/08 - 8/31/10				
Location of Project: Washington University				
Person-Months Per Year Committed to the Project. Cal: Acad: Sumr: 0.7				
Support: ☐ Current ☒ Pending ☐ Submission Planned in Near Future ☐ *Transfer of Support				
Project/Proposal Title:				
ETBC: Hidden Iron Oxide Redox Processes During Biogeochemical Iron Cycling: Control on Nanoscale Transformations and the Fate of Contaminants				
Source of Support: NSF/GEO-BIO				
Total Award Amount: $340,505 Total Award Period Covered: 9/1/08 - 8/31/11				
Location of Project: Washington University				
Person-Months Per Year Committed to the Project. Cal: Acad: Sumr: 1.0				
Support: ☐ Current ☒ Pending ☐ Submission Planned in Near Future ☐ *Transfer of Support				
Project/Proposal Title:				
Phosphate Controls on Subsurface Uranium Fate and Transport: Connecting Molecular-Scale and Sediment-Scale Processes (with co-PIs Giammar (Washington University) and Wellman (PNNL)				
Source of Support: Department of Energy				
Total Award Amount $931,543 (Wash. U. portion) Total Award Period Covered: 9/1/08 – 8/31/11				
Location of Project: Washington University				
Person-Months Per Year Committed to the Project. Cal: Acad: Sumr: 1.0				
Support: ☐ Current ☐ Pending ☐ Submission Planned in Near Future ☐ *Transfer of Support				
Project/Proposal Title:				
Source of Support:				
Total Award Amount Total Award Period Covered:				
Location of Project:				
Person-Months Per Year Committed to the Project. Cal: Acad: Sumr:				